Cell Research

www.nature.com/cr
www.cell-research.com

ARTICLE

Ttm50 facilitates calpain activation by anchoring it to calcium stores and increasing its sensitivity to calcium

Elsayed Metwally[1,2,3], Guoli Zhao[1,4,5], Qifu Wang[1] and Yong Q. Zhang[1,2]

Calcium-dependent proteolytic calpains are implicated in a variety of physiological processes, as well as pathologies associated with calcium overload. However, the mechanism by which calpain is activated remains elusive since intracellular calcium levels under physiological conditions do not reach the high concentration range required to trigger calpain activation. From a candidate screening using the abundance of the calpain target glutamate receptor GluRIIA at the *Drosophila* neuromuscular junction as a readout, we uncovered that calpain activity was inhibited upon knockdown of Ttm50, a subunit of the Tim23 complex known to be involved in the import of proteins across the mitochondrial inner membrane. Unexpectedly, Ttm50 and calpain are co-localized at calcium stores Golgi and endoplasmic reticulum (ER), and Ttm50 interacts with calpain via its C-terminal domain. This interaction is required for calpain localization at Golgi/ER, and increases calcium sensitivity of calpain by roughly an order of magnitude. Our findings reveal the regulation of calpain activation by Ttm50, and shed new light on calpain-associated pathologies.

Cell Research (2021) 31:433–449; https://doi.org/10.1038/s41422-020-0388-4

INTRODUCTION

Calpains are calcium-activated cytoplasmic cysteine proteases that are ubiquitously expressed in various tissues and functionally active at neutral pH.[1,2] As hundreds of calpain target proteins that can be cleaved by calpain have been identified,[3] calpain activity has to be tightly regulated not only by intracellular calcium, but also by the endogenous inhibitor calpastatin. Overactivation of calpains has been well established in brain injury and neurodegeneration with calcium overload including ischemia and Alzheimer's disease.[4–6] For example, the activation ratio of calpain 1 is increased 3-fold in the prefrontal cortex from patients with Alzheimer's disease compared with controls.[4] Activation of calpains leads to the cleavage of p35 to p25 that leads to the prolonged activation and mislocalization of cyclin-dependent kinase 5 (cdk5) resulting in neuronal death.[5]

While the majority of previous studies have focused on the role of calpains in pathologies involving calcium overload, recent genetic studies revealed critical roles for calpains in physiology and normal development. In mammals, mutations in calpain 1 lead to hereditary spastic paraplegia and cerebellar ataxia.[7,8] In *Drosophila*, calpain activity is developmentally regulated during dendrite pruning due to compartmentalized calcium transits in neurons.[9] More recently, we showed that calpains cleave the glutamate receptor GluRIIA at *Drosophila* neuromuscular junction (NMJ) synapses during development.[10] However, how calpain activity is regulated in pathological and physiological processes remains to be elucidated.

Calpain 1 and calpain 2, the most well-characterized calpain family members, are activated in vitro by micromolar (~50 μM) and millimolar (~1 mM) concentrations of calcium, respectively.[3,11] However, the physiological intracellular calcium concentration in resting stage is ~100 nanomolar (nM) when averaged over a whole cell and never achieves a level that is sufficient to activate calpains in in vitro assays.[12,13] Thus, exactly how calpains are activated in vivo in the presence of physiological levels of calcium remained poorly understood.[14,15] Although various calpain activators such as acyl-CoA-binding protein and phospholipids are reported to increase the calcium sensitivity of these proteases,[3,16] activation by these activators has not been demonstrated in vivo, and the mechanism of activation remains unclear. Herein, we discovered that tiny tim 50 (Ttm50), a subunit of the Tim23 complex that participates in the import of proteins across the inner membrane of mitochondria to the matrix, co-localizes and interacts with calpain. This interaction between Ttm50 and calpain is required for calpain localization at calcium stores, Golgi and endoplasmic reticulum (ER), and increases calpain sensitivity to calcium, thereby facilitating calpain activation.

RESULTS

Ttm50 is identified as a positive calpain regulator

Given the critical role of calpain activity in a range of physiological and pathological processes, we set out to identify proteins that regulate calpain activity. In our previous study,[10] we discovered that individual postsynaptic knockdown of calpains, or 15 other genes in muscles by *C57-Gal4* was associated with similar

[1]State Key Laboratory for Molecular and Developmental Biology, CAS Center for Excellence in Brain Science and Intelligence Technology, Institute of Genetics and Developmental Biology, Chinese Academy of Sciences, Beijing 100101, China and [2]International College, University of Chinese Academy of Sciences, Beijing 10080, China
Correspondence: Yong Q. Zhang (yqzhang@genetics.ac.cn)
[3]Present address: Department of Cytology and Histology, Faculty of Veterinary Medicine, Suez Canal University, Ismailia 41522, Egypt
[4]Present address: F. M. Kirby Neurobiology Center, Boston Children's Hospital, Boston, MA 02115, USA
[5]Present address: Department of Neurobiology, Harvard Medical School, Boston, MA 02115, USA
These authors contributed equally: Elsayed Metwally, Guoli Zhao

Received: 9 February 2020 Accepted: 20 July 2020
Published online: 26 August 2020

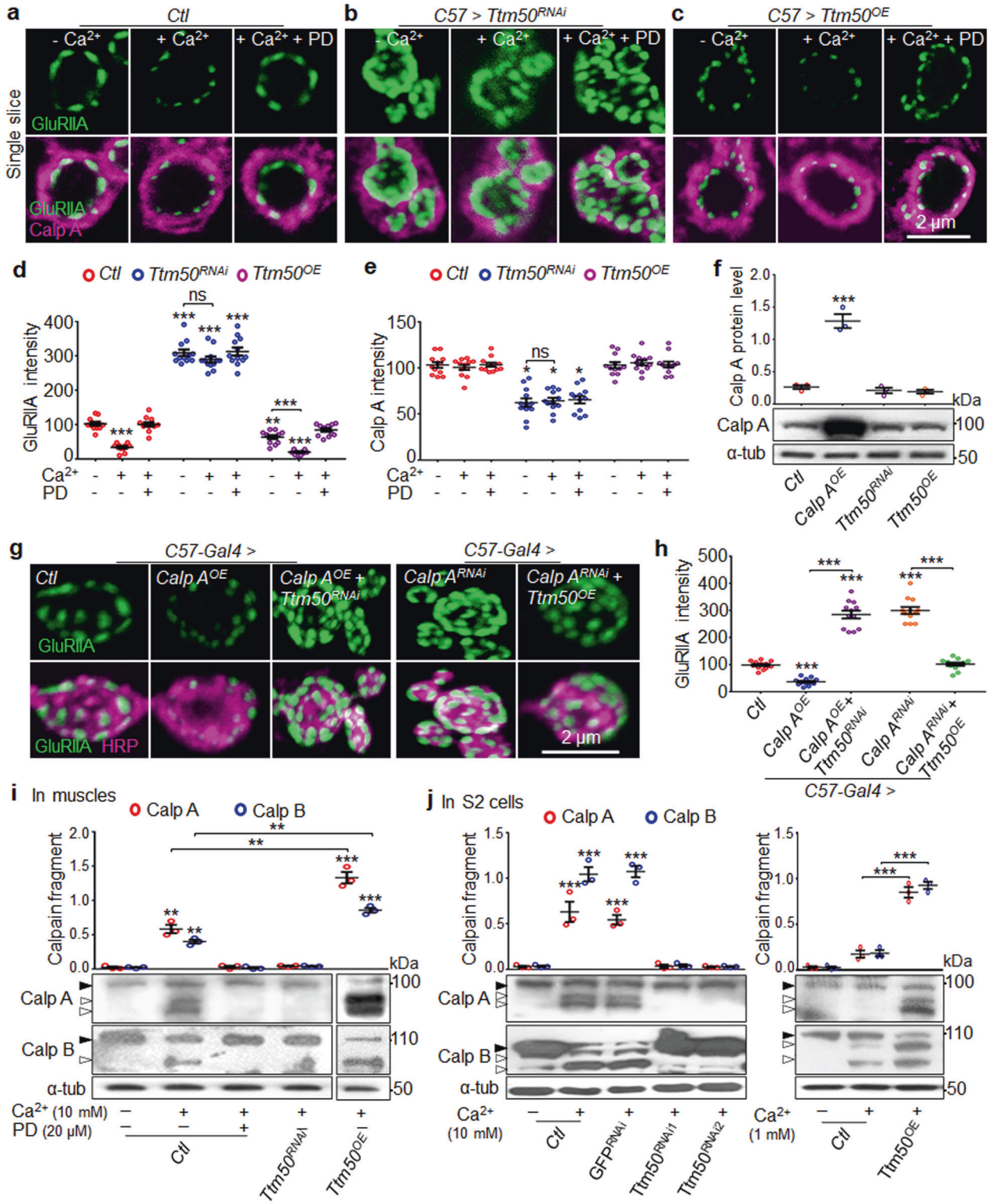

upregulation of GluRIIA at NMJ termini. We therefore explored whether any of the 15 positive genes might work with calpain to downregulate GluRIIA levels. Based on our previous finding that calcium treatment reduces GluRIIA abundance at synapses via calpain, as the reduction of GluRIIA was inhibited after treatment with PD150606, a cell-permeable calpain inhibitor[10] (Fig. 1a, d), we examined the effects of the 15 candidate genes on calcium-induced GluRIIA downregulation. We hypothesized that any gene that regulates calcium-dependent downregulation of GluRIIA might also affect calpain activity. Among the 15 candidate genes tested, we found that postsynaptic knockdown of *p32*, *Hsp60*, and *Ttm50* in muscles abolished calcium-induced GluRIIA downregulation in the presence of 1 mM calcium (Fig. 1b, d; Supplementary information, Fig. S1a).

Ttm50, p32, and Hsp60 proteins are functionally unrelated, but all are reportedly localized to mitochondria.[17–20] To further

Fig. 1 Ttm50 is a positive calpain regulator. a–c Calcium-induced downregulation of GluRIIA (**a**) is attenuated by Ttm50 knockdown (**b**) and enhanced by Ttm50 overexpression (**c**). Representative images of NMJ synapses from different genotypes co-stained with anti-GluRIIA (green) and anti-Calp A (magenta) antibodies. Muscle cells were treated with dimethylsulfoxide (DMSO) vehicle, calcium, and calcium plus calpain inhibitor PD150606. 10 μM ionomycin was used to stimulate calcium influx. Scale bar, 2 μm. See also Supplementary information, Fig. S1 for genetic screening of calpain regulators at NMJ synapses. **d**, **e** Quantitative analysis of the fluorescence intensity of GluRIIA (**d**) and Calp A (**e**) from different genotypes following different treatments. $n = 12$ NMJs (one NMJ for each larva), ns, no significance, $^{*}P < 0.05$, $^{**}P < 0.01$ and $^{***}P < 0.001$ by one-way ANOVA with Tukey's post hoc test and student's *t*-test. Data are presented as means ± SEM. **f** Representative immunoblots of muscles from different genotypes probed with anti-Calp A antibody. α-tubulin was used as a loading control. Scatter plot graph shows relative levels of Calp A in indicated genotypes. $n = 3$, $^{***}P < 0.001$ by one-way ANOVA with Tukey's post hoc test. Data are presented as means ± SEM. **g**, **h** Ttm50 positively regulates calpain activity. Representative images of NMJ synapses from different genotypes co-stained with anti-GluRIIA (green) and anti-HRP (magenta) antibodies (**g**). Scale bar, 2 μm. Quantitative analysis of the fluorescence intensity of GluRIIA from different genotypes (**h**). $n = 12$ NMJs, ns, no significance, $^{***}P < 0.001$ by one-way ANOVA with Tukey's post hoc test and student's *t*-test. Data are presented as means ± SEM. See also Supplementary information, Fig. S2 for mitochondrial and cytoplasmic calcium levels in larval muscles and S2 cells upon knockdown of *Ttm50, p32* and *Hsp60*. See also Supplementary information, Fig. S3 for Ttm50-mediated calpain activation during dendritic pruning of sensory neurons. **i**, **j** Knockdown of Ttm50 inhibits calpain activity while overexpression of Ttm50 increases calpain activity in muscles and in S2 cells. Lysates of muscles (**i**) and S2 cells (**j**) expressing altered levels of Ttm50, treated with calcium at different concentrations, were analyzed by western blotting with anti-calp A and anti-calp B antibodies. α-tubulin was used as a loading control. Black arrowheads indicate full-length calpains and open arrowheads indicate autolyzed calpain fragments. Scatter plot graphs show relative levels of Calp A and Calp B fragments in indicated genotypes. $n = 3$, $^{**}P < 0.01$, $^{***}P < 0.001$ by one-way ANOVA with Tukey's post hoc test and student's *t*-test. Data are presented as means ± SEM.

examine whether regulation of GluRIIA by these genes is dependent on calcium, we treated muscle cells with a higher concentration of calcium (5 mM) and found that knockdown of *Ttm50* but not *p32* or *Hsp60* inhibited calcium-induced downregulation of GluRIIA (Supplementary information, Fig. S1b). This suggests that Ttm50 is required for calcium-dependent downregulation of GluRIIA, while p32 and Hsp60 might regulate calpain sensitivity to calcium, calcium homeostasis, or both. To verify these possibilities, we measured the cytoplasmic calcium concentration by Fluo-4AM staining upon ionomycin-induced calcium release from intracellular organelles and mitochondrial calcium concentration by Rhod-2AM staining, and found that the calcium concentration in both cytoplasm and mitochondria of muscles was decreased when p32 or hsp60 were knocked down, but knockdown of Ttm50 had no such an effect (Supplementary information, Fig. S2a–d). Consistently, the calcium level in the cytoplasm and mitochondria of S2 cells remained normal as in control upon ionomycin treatment when Ttm50 was knocked down or overexpressed (Supplementary information, Fig. S2e–h), supporting that Ttm50 does not affect cellular calcium homeostasis at least under the conditions we examined.

As with calpain overexpression, Ttm50 overexpression in muscles reduced GluRIIA levels in a calcium-dependent manner. The relative abundance of GluRIIA in *C57-Gal4>Ttm50* was significantly reduced upon calcium treatment compared with untreated samples (Fig. 1c, d). While the intensity of calpain A at NMJ synapses was significantly reduced upon Ttm50 knockdown (Fig. 1b, e), the total calpain A level remained normal when Ttm50 was knocked down or overexpressed (Fig. 1f). Among the three candidates, we focused on Ttm50 because this protein was the only one that regulates calcium-dependent GluRIIA downregulation without interfering with calcium levels, and therefore a possible genuine regulator of calpain activity.

Ttm50 positively regulates calpain activity

To better understand how Ttm50 regulates calpain activity in vivo, we investigated the interaction between calpain and Ttm50 in the regulation of GluRIIA, and found that calpain A overexpression-induced GluRIIA reduction at NMJ synapses was attenuated by RNAi knockdown of Ttm50 (Fig. 1g, h). Conversely, partial calpain A knockdown-induced upregulation of GluRIIA, as previously documented,[10] was inhibited by Ttm50 overexpression (Fig. 1g, h). In addition to the downregulation of GluRIIA at NMJ synapses, calpains are also involved in dendrite pruning as a result of compartmentalized calcium transits in *Drosophila* neurons.[9] We therefore hypothesized that calcium transients and Ttm50 may act cooperatively to promote calpain-mediated dendrite pruning. Indeed, we found that calpain activity is also tightly and positively regulated by Ttm50 in promoting dendrite pruning of sensory neurons (Supplementary information, Fig. S3).

Activation of native calpain involves autolytic conversion from an inactive pro-enzyme to an active form that can cleave its substrates.[21,22] We therefore investigated the effect of Ttm50 on calpain activation using calpain autolytic fragments as a readout. Autolysis of both calpains A and B in muscles became apparent upon calcium treatment, and production of calpain fragments was inhibited by the calpain inhibitor PD150606 (Fig. 1i). As expected, knockdown of Ttm50 effectively inhibited the production of calpain autolytic fragments, while overexpression of Ttm50 showed the opposite effect in muscle cells (Fig. 1i). We further verified the role of Ttm50 in promoting calpain activity in S2 cells. Independent Ttm50 double-stranded RNAs (dsRNAs), but not control green fluorescence protein (GFP) dsRNAs, inhibited calpain A and calpain B autolysis, while overexpression of Ttm50 increased calpain autolytic activity in S2 cells (Fig. 1j). Together, these results demonstrate that Ttm50 is a positive regulator of calpain activity both in vivo and in S2 cells.

Ttm50 co-localizes with calpain at Golgi and ER

Since calpain activity was found to be tightly regulated by Ttm50, we hypothesized that these proteins might co-localize and interact with each other. To determine the localization of endogenous Ttm50, we generated a rabbit polyclonal antibody against amino acid residues 81–97 and 207–223 of Ttm50. The specificity of Ttm50 antibody and the efficacy of Ttm50 RNAi were verified by immunostaining and western blot analysis (Supplementary information, Fig. S4a–c). To determine if there was co-localization of Ttm50 and calpain, we generated a hemagglutinin (HA) knockin at the C-terminus of endogenous Ttm50 (antibodies for both Ttm50 and calpain A were generated in rabbits). Co-immunostaining analysis showed that Ttm50-HA and calpain A did indeed overlap at NMJs and at distinct puncta in muscles (Supplementary information, Fig. S4d, e, g). Overexpressed HA- or Myc-Ttm50 was also substantially co-localized to various extents with calpain A at distinct puncta in muscles and S2 cells (Supplementary information, Fig. S4e–g).

Endogenous calpain A and Ttm50 proteins appeared to be localized to GM130-positive Golgi and KDEL-positive ER, but they were rarely localized to mitochondria (positive for MitoTracker red) in muscle cells of *Drosophila* (Fig. 2a–c). Consistently, we found that overexpressed calpain and Ttm50 were substantially co-localized at Golgi/ER in S2 cells (Supplementary information, Fig. S4h–j). However, Ttm50 and its homologs in other organisms are reported to function as a subunit of the Tim23 complex

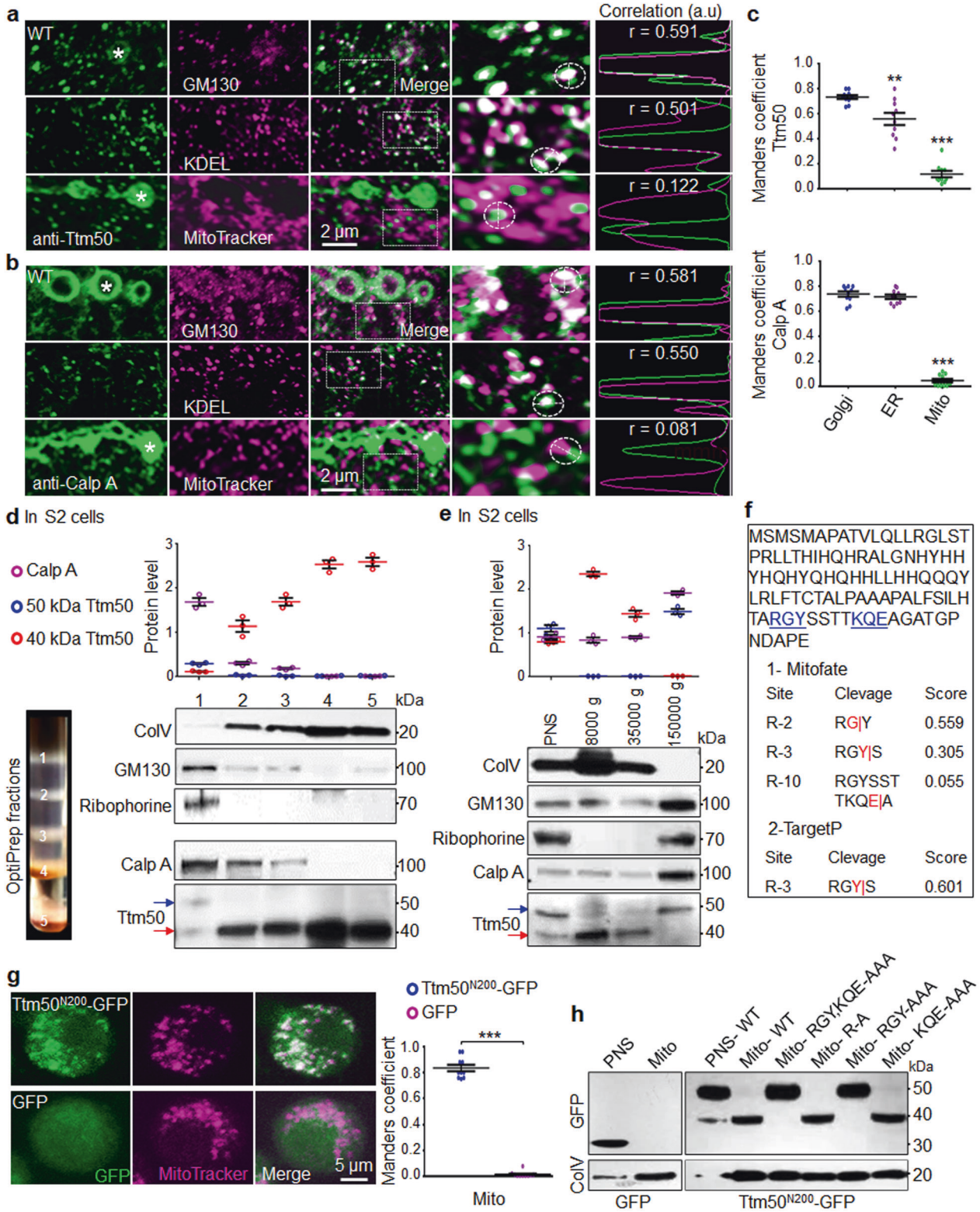

located in the mitochondrial inner membrane.[20,23] To address this apparent discrepancy, we tested whether Ttm50 was localized in mitochondria using fractionation assays. S2 cell lysates were subjected to Optiprep velocity gradient centrifugation and differential velocity centrifugation. The resulting fractions obtained from both gradients were subjected to western blot analysis using antibodies against proteins associated with mitochondria, Golgi and ER (Fig. 2d, e). Consistent with previous reports,[24,25] mitochondria were primarily resided in Optiprep gradient fractions 2, 3, 4, and 5, and in the pellets obtained by velocity centrifugation at 8000× *g* and 35,000× *g*, as detected by antibodies against cytochrome oxidase (ColV) for mitochondria. Meanwhile, Golgi and ER proteins were detected in fraction 1 by Optiprep assay, and were largely enriched in the pellet after

Fig. 2 Ttm50 co-localizes with calpain A at Golgi/ER. a, **b** Endogenous Ttm50 and calpain localize at Golgi/ER. Representative images of wild-type muscles co-stained with anti-Ttm50 (**a**) or Calp A (**b**) together with a Golgi marker anti-GM130, an ER marker anti-KDEL and a mitochondrial marker mitoTracker red (magenta). White Asterisks in **a** and **b** indicate NMJ synapses. Pearson correlation coefficient (*r*) is indicated. Scale bar, 2 μm. **c** Manders coefficient as a measure of co-localization of calpain A and Ttm50 with Golgi, ER and mitochondria. $n = 10$ larval muscle cells, $^{**}P < 0.01$, $^{***}P < 0.001$ by one-way ANOVA with Tukey's post hoc test. Data are presented as means ± SEM. See also Supplementary information, Fig. S4 for Ttm50 and Calp A localization at neuromusculture and in S2 cells. **d** Ttm50 displays dual localization in both mitochondria and Golgi/ER. Representative immunoblots are shown for five fractions of S2 cell lysates using OptiPrep velocity centrifugation with antibodies against CoIV, GM130, Ribophorine, Calp A and Ttm50. **e** Fractions of S2 cell lysates after differential velocity centrifugation were subjected to western blot analysis with the same antibodies. Equal amounts of protein from each fraction were separated by SDS-PAGE. The blue arrow indicates full-length (50 kDa) extra-mitochondrial Ttm50, whereas the red arrow denotes 40 kDa mitochondrial Ttm50. In **d** and **e**, scatter plot graphs show relative levels of indicated proteins in different fractions. $n = 3$. **f**–**h** Ttm50 is imported into mitochondria by the N-terminal MTS which is cleaved at the RGY site. Analysis using Mitofates and TargetP predicted RGY and KQE as recognition sites for MTS cleavage (**f**). Representative images of S2 cells expressing $Ttm50^{N200}$-GFP or GFP co-stained with MitoTracker red (**g**). Scale bar, 5 μm. Manders Coefficient as a measure of co-localization of Ttm50 and mitochondria. $n = 10$ S2 cells, $^{***}P < 0.001$ by student's *t*-test. Data are presented as means ± SEM. Representative immunoblots of S2 cells expressing GFP alone, wild-type $Ttm50^{N200}$-GFP, and $Ttm50^{N200}$-GFP carrying various mutations in the putative cleavage sites probed with anti-GFP and anti-CoIV (a marker for mitochondria) after fractionation into post-nuclear supernatant (PNS) and mitochondrial pellet (Mito) fractions (**h**).

150,000× *g* centrifugation, as detected by antibodies against GM130 for Golgi and ribophorine for ER (Fig. 2d, e). Calpain A was predominantly associated with Golgi and ER, but rarely with mitochondria (Fig. 2d, e), consistent with a previous report that mammalian calpains are associated with ER and Golgi.[26] Full-length Ttm50 (50 kDa) was present in Golgi and ER fractions, while the shorter 40 kDa Ttm50 isoform was detected in the mitochondrial fraction (Fig. 2d, e). Western blot analysis of both muscles and S2 cells showed that these two bands were specific for Ttm50 (Supplementary information, Fig. S4b, c). The discrepancy of Ttm50 localization at mitochondria might be caused by the fact that the epitope recognized by anti-Ttm50 might be hidden within the Ttm23 complex during fixation for immunostaining but become accessible when the protein is linearized for western blotting. Together with a lack of evidence supporting alternative splicing of *Ttm50* in multiple RNA-seq datasets of *Drosophila* (http://flybase.org/), these results indicate that full-length Ttm50 in Golgi and ER might be subjected to proteolytic cleavage to generate a smaller 40 kDa isoform in mitochondria.

The N-terminus of Ttm50 includes a mitochondria targeting sequence

Many mitochondrial proteins carry an N-terminal mitochondria-targeting sequence (MTS) that is removed by specific peptidases in the mitochondrial matrix.[27] To determine if the N-terminus of Ttm50 contains an MTS, we searched for potential MTS cleavage sites in Ttm50 using bioinformatics software. Analysis with Mitofates[28] and TargetP[29] predicted the presence of an N-terminal MTS with putative cleavage sites, as shown in Fig. 2f. Cleavage of the MTS could theoretically result in a C-terminal Ttm50 fragment of 40 kDa, as shown in Fig. 2d, e. Indeed, the N-terminal 200 amino acids (aa) of Ttm50 was sufficient to target GFP to mitochondria in S2 cells (Fig. 2g). Consistent with cleavage of the MTS, the mitochondria-enriched form of $Ttm50^{N200}$-GFP (40 kDa) was smaller than the unprocessed $Ttm50^{N200}$-GFP (50 kDa; N-terminal 200 aa of Ttm50 plus 238 aa GFP) detected in the post-nuclear supernatant (PNS) fraction (Fig. 2h).

MTS cleavage sites have been extensively analyzed according to the position of an arginine (R) in the N-terminus.[30] The R-2 motif (Rx*x) and the R-3 motif (Rx(Y/x)*x) might be cleaved by mitochondrial processing peptidase (MPP), while the third R-10 motif, Rx(F/L/I)xx(S/T/G)xxxx*x, might be cleaved by octapeptidyl aminopeptidase (Oct1).[30,31] Consistently, bioinformatics analysis showed that putative MPP cleavage sites in the presequence of Ttm50 are located at G81 of the R-2 motif RG*Y and Y82 at the R-3 motif RGY*S, while the putative cleavage site for Oct1 is located at E89 of the R-10 motif RGYSSTTKQE*A (Fig. 2f). We then performed mutational analysis of the putative cleavage sites, and the results are shown in Fig. 2h. S2 cells expressing wild-type $Ttm50^{N200}$-GFP and mutated $Ttm50^{N200}$-GFP were fractionated into PNS and mitochondrial fractions, electrophoresed, and probed with anti-GFP antibody. Wild-type, R80-A and KQE-AAA mutants of $Ttm50^{N200}$, but not RGY-AAA or RGY/KQE-AAA/AAA mutants, generated 40 kDa cleavage products (Fig. 2h), demonstrating that Ttm50 is cleaved at position G81 and/or Y82. Taken together, these results support the notion that Ttm50 is imported from the cytoplasm to mitochondria followed by MTS cleavage.

Ttm50 interacts with calpain via its C-terminus

The co-localization of Ttm50 with calpain at ER and Golgi suggests that they may interact with each other. To examine this possibility, we tested whether Ttm50 physically interacted with calpains by co-immunoprecipitation (Co-IP) analysis of muscle lysates. Ttm50 did indeed interact with calpain A, and the interaction was enhanced by calcium treatment (Fig. 3a). A physical interaction between Ttm50 and calpains was confirmed by Co-IP in S2 cells (Fig. 3b). These interactions were specific since IP by a non-specific IgG did not yield a positive signal for target proteins (Fig. 3a, b). We note that only the full-length, ER/Golgi-localized Ttm50, but not the 40 kDa mitochondrial Ttm50, was positive for Co-IP by anti-calpain A antibody (Fig. 3a).

Furthermore, we mapped the domains mediating the interaction between calpain A and Ttm50, and found that the domain IV of calpain A interacted with the C-terminal TFIIF-interacting CTD phosphatase 1 (FCP1) domain of Ttm50 (Supplementary information, Fig. S5a–e). Moreover, domain IV of calpain A was required for its localization at GM130-positive Golgi and KDEL-positive ER in S2 cells (Supplementary information, Fig. S5f–i).

To further support a direct interaction between calpain and Ttm50 in vitro, we conducted in vitro binding assays between glutathione-S-transferase (GST)-calpain A and His-tagged Ttm50 both affinity purified from *Escherichia coli*. We found that Ttm50 was not recovered from beads conjugated with GST alone, while Ttm50 and the FCP1 domain, but not the FCP1-deleted Ttm50, were recovered from GST-calpain A beads (Fig. 3c). Reciprocally, His-tagged Ttm50 and FCP1 but not FCP1-deleted Ttm50 from *E. coli* immobilized on Ni-NTA resin successfully pulled down GST-calpain A but not GST alone (Fig. 3d). These results further indicate that Ttm50 directly interacts with calpain A via the C-terminal FCP1 and domain IV, respectively.

To further identify residues in the FCP1 domain that are crucial for the interaction between calpain and Ttm50, we first determined which region in the FCP1 domain interacts with calpain A. Two regions of FCP1, each comprising 72 residues (amino acids 224–295 and 296–367), were expressed in S2 cells. Cell lysates were incubated with *E. coli*-derived His-tagged calpain A immobilized on Ni-NTA resin. Peptides containing residues 224–295 but not residues 296–367 of FCP1 were associated with

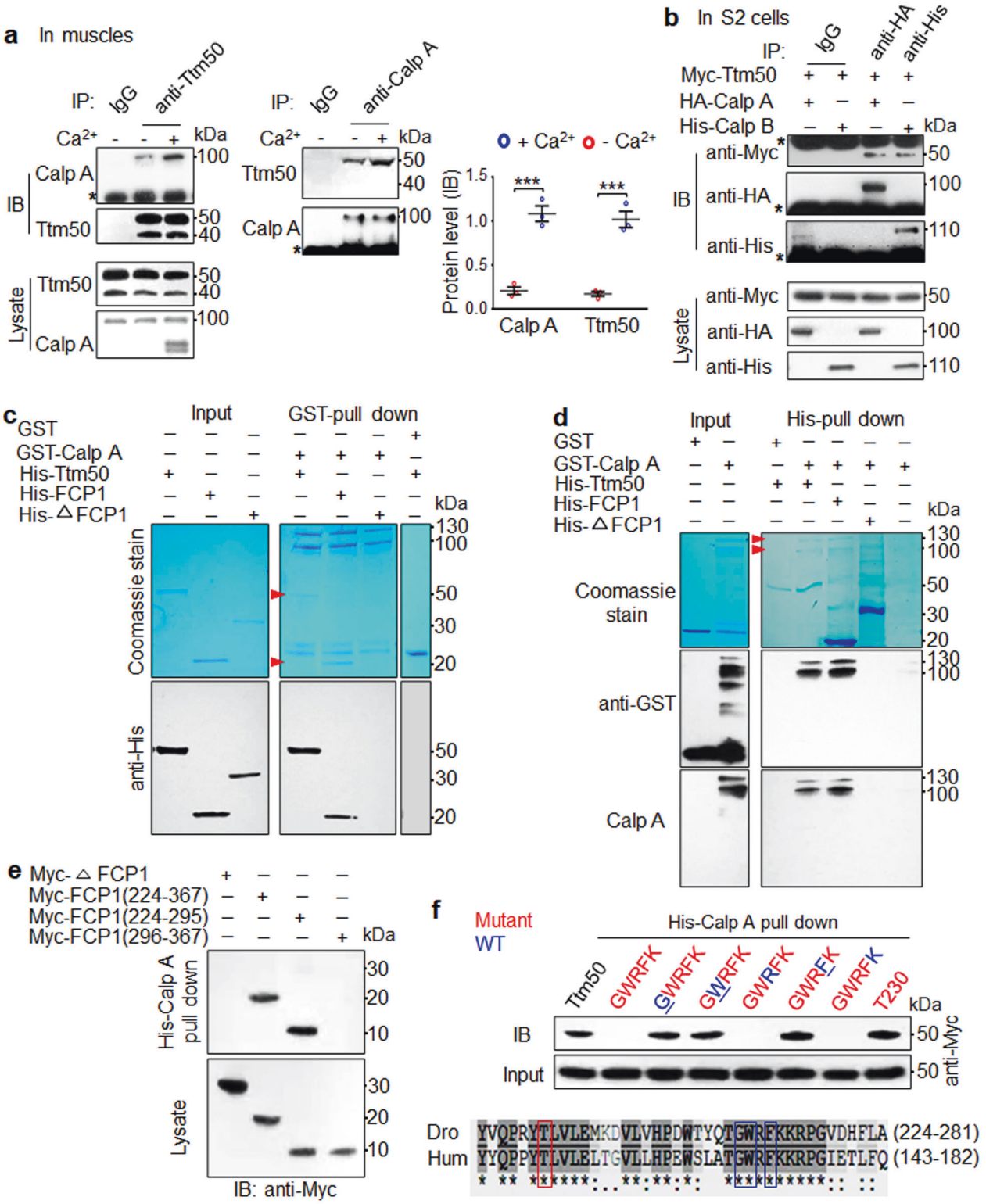

calpain A (Fig. 3e). To narrow down the sub-region within residues 224–295 of FCP1 that was required for the Ttm50–calpain interaction, we performed site-directed alanine substitution for every 10 residues, as shown in Supplementary information, Fig. S6a. Compared with wild-type Ttm50, mutation to 10 alanines in region 5 (WTYQTGWRFK) and region 6 (GWRFKKRPGV) abolished the Ttm50–calpain interaction (Supplementary information, Fig. S6b). Mutating the overlapping GWRFK sequence in regions 5 and 6 but not region-specific WTYQT or KRPGV abolished interaction with calpain A (Supplementary information, Fig. S6c). However, mutation of single residues within the GWRFK motif did not disrupt the interaction. Further mutational analysis showed that the single hydrophobic residues G249, W250 and F252, but not positively charged residues R251 and K253 in the

Fig. 3 Ttm50 interacts with calpain via the C-terminal fragment. a, **b** Calpain A and B interact physically with Ttm50 in vivo and in S2 cells in a calcium-dependent manner. Lysates of muscles treated with or without calcium were subjected to Co-IP with anti-Ttm50 or anti-Calp A followed by western blot analysis with the indicated antibodies (**a**). Scatter plot graph shows relative levels of immunoprecipitated Calp A and Ttm50. $n = 3$, $^{***}P < 0.001$ by student's *t*-test. Data are presented as means ± SEM. Lysates of S2 cells co-expressing Myc-Ttm50 and HA-Calp A or His-Calp B were subjected to Co-IP with anti-HA or anti-His antibodies, followed by western blotting with indicated antibodies (**b**). Asterisks indicate the IgG heavy chain at 55 kDa. See also Supplementary information, Fig. S5 for interactions of Flag-tagged calpain A and Myc-tagged Ttm50 variants. **c**, **d** Ttm50 directly interacts with calpain via FCP1 in vitro. His-tagged proteins purified from *E. coli* were incubated with glutathione-sepharose beads loaded with GST or GST-Calp A. Immobilized proteins were then subjected to western blot analysis using anti-His antibody (**c**). GST-Calp A or GST proteins were incubated with purified His-tagged proteins immobilized on Ni-NTA resin. Immobilized proteins were subjected to immunoblotting with anti-GST and anti-Calp A (**d**). The red arrowheads indicate specific proteins pulled down by GST (**c**) and His (**d**). **e** S2 lysates expressing Myc-tagged FCP1-deleted Ttm50, FCP1 (224–367 aa), FCP1 (224–295 aa) and FCP1 (296–367aa) were pulled down by *E. coli*-derived His-calp A immobilized on Ni-NTA resin. **f** Hydrophobic G249, W250 and F252 residues in the GWRFK motif of Ttm50 are each sufficient for Ttm50–calpain interaction. Wild-type (control) and various mutated Ttm50 constructs were transfected into S2 cells and the resulting lysates were incubated with *E. coli*-derived His-calp A immobilized on Ni-NTA resin, followed by immunoblotting with anti-Myc antibody. Blue boxes in the lower panel indicate critical residues mediating the Ttm50–calpain interaction in *Drosophila* Ttm50 (Accession No. NP_570027) and human Tim50 (Accession No. NP_001001563.2). The red box indicates T230 which is associated with mitochondrial function. See also Supplementary information, Fig. S6 for identification of crucial residues involved in the Ttm50–calpain interaction.

GWRFK motif were sufficient for the Ttm50–calpain interaction (Fig. 3f). As another control, Ttm50 containing T230A point mutation did not abolish the Ttm50–calpain interaction (Fig. 3f). T230A is the equivalent site of human Tim50 T252M, a mutation associated with mitochondrial dysfunction in human,[32] which is named based on the nuclear isoform of Tim50, and the counterpart on mitochondrial isoform is T149M (UniProt. Q3ZCQ8). These results demonstrate that the GWRFK motif mediates the interaction between Ttm50 and calpain.

Disruption of the Ttm50–calpain interaction inhibits calpain activity and localization to ER in S2 cells

If binding of Ttm50 to calpain A is functionally relevant, introducing point mutations in the GWRFK motif that interfere with calpain A binding should compromise calpain activity and localization in cells. Indeed, expression of wild-type or T230A Ttm50 but not Ttm50 mutant carrying GWRFK to AAAAA mutations enhanced GluRIIA cleavage and calpain autolysis in S2 cells (Fig. 4a, b). Since Ttm50 directly interacts with calpain A via its C-terminal part (Fig. 3), we hypothesized that overexpression of the FCP1 domain, which is sufficient to bind calpain, may disrupt the interaction between Ttm50 and calpain in a dominant negative manner in cultured cells. This was indeed the case (Fig. 4b; Supplementary information, Fig. S6d). The amount of Ttm50 co-precipitated with calpain A was reduced in S2 cells expressing Myc-FCP1 (Fig. 4b). Conversely, the amount of calpain A co-precipitated with Ttm50 was substantially decreased in S2 cells expressing Myc-FCP1 (Supplementary information, Fig. S6d). By contrast, expressing Myc-tagged FCP1-deleted Ttm50 as well as mutant FCP1 domain harboring GWRFK-AAAAA mutations but not T230A single mutation did not affect the Ttm50–calpain interaction (Fig. 4b). However, expression of wild-type or T230A FCP1 but not FCP1 mutant carrying GWRFK quintuple mutations increased calpain autolysis in the presence of 1 mM calcium (Fig. 4b), indicating that FCP1 is sufficient for calpain activation.

To determine whether the Ttm50–calpain interaction regulates calpain localization, we examined calpain A localization upon expression of different variants of Ttm50. In S2 cells, endogenous calpain A was evenly distributed in the cytoplasm (Fig. 4c), similar to calpain 2 in mammalian cells.[26,33] However, when S2 cells were treated with ionomycin, the diffused cytoplasmic calpain A was re-localized to ER (we were unable to do co-staining between calpain A and Golgi as both antibodies were generated in rabbits), and this re-localization was dependent on Ttm50 since knockdown of Ttm50 disrupted the process (Fig. 4c, d). As expected, expression of Ttm50 harboring GWRFK to AAAAA mutations did not rescue Ttm50 RNAi-induced mislocalization of endogenous calpain upon calcium treatment, whereas overexpression of wild-type and the T230A mutant Ttm50 did (Fig. 4c, d).

Since Ttm50 is a subunit of the Tim23 complex involved in mitochondrial function, we wondered whether the GWRFK motif that mediates the Ttm50–calpain interaction could affect mitochondrial function. To investigate this possibility, we performed JC-1 staining to monitor the mitochondrial membrane potential (MMP) because Ttm50 plays a role in maintaining the permeability barrier of the mitochondrial inner membrane in yeast and *Drosophila*.[23,34] JC-1 dye exhibits potential-dependent accumulation in mitochondria, indicated by a fluorescence emission shift from green (~529 nm) to red (~590 nm); the higher the shift of fluorescence intensity, the higher MMP.[35] We first established that S2 cell mitochondria behave similarly to mammalian mitochondria in terms of maintaining an electrochemical proton gradient by JC-I staining (Supplementary information, Fig. S6e). As expected, RNAi knockdown of Ttm50 in S2 cells resulted in a significant decrease in JC-1 staining, while overexpression of wild-type Ttm50 and GWRFK-AAAAA mutant Ttm50 but not T230A mutant Ttm50 led to an increased JC-1 abundance (Fig. 4e, f). Moreover, overexpression of wild-type and the GWRFK-AAAAA mutant Ttm50 but not the T230A mutant Ttm50 rescued the phenotype of reduced JC-1 staining caused by Ttm50 RNAi knockdown (Fig. 4e, f). These mutational analysis results support distinct dual functions for Ttm50, namely interacting with and activating calpain via the GWRFK motif, and acting as a subunit of the Tim23 complex.

Ttm50 increases calpain sensitivity to calcium in vitro

To check if Ttm50 was sufficient to promote calpain activation in vitro, we incubated Ttm50 purified from *E. coli* with immunoprecipitated calpain A from S2 cells for 1 h at different calcium concentrations. We used calpain autolysis as an indicator of calpain activation. As shown in Fig. 5a, when 1 μg of IgG was added as a control, autolysis of calpain A did not occur unless calcium was added at a final concentration of 5 mM (Fig. 5a, b). Interestingly, when purified Ttm50 was added to the reaction, the rate of autolysis increased in a dose-dependent manner. Specifically, compared with control (without Ttm50), treated with 5 mM calcium, the autolytic fragments of calpain A was more than trebled upon addition of 0.2 μg Ttm50, while addition of 0.4 μg Ttm50 led to complete calpain autolysis within 1 h (Fig. 5a, b). These results indicate that Ttm50 increases calpain sensitivity to calcium. We further found that the FCP1 domain of Ttm50 but not FCP1-deleted Ttm50 was also sufficient to promote calpain activity in vitro (Fig. 5c, d), in support of the physical interaction between calpain and Ttm50 via the FCP1 domain. These results support that Ttm50 increases calpain sensitivity to calcium, thereby facilitating calpain proteolytic activity.

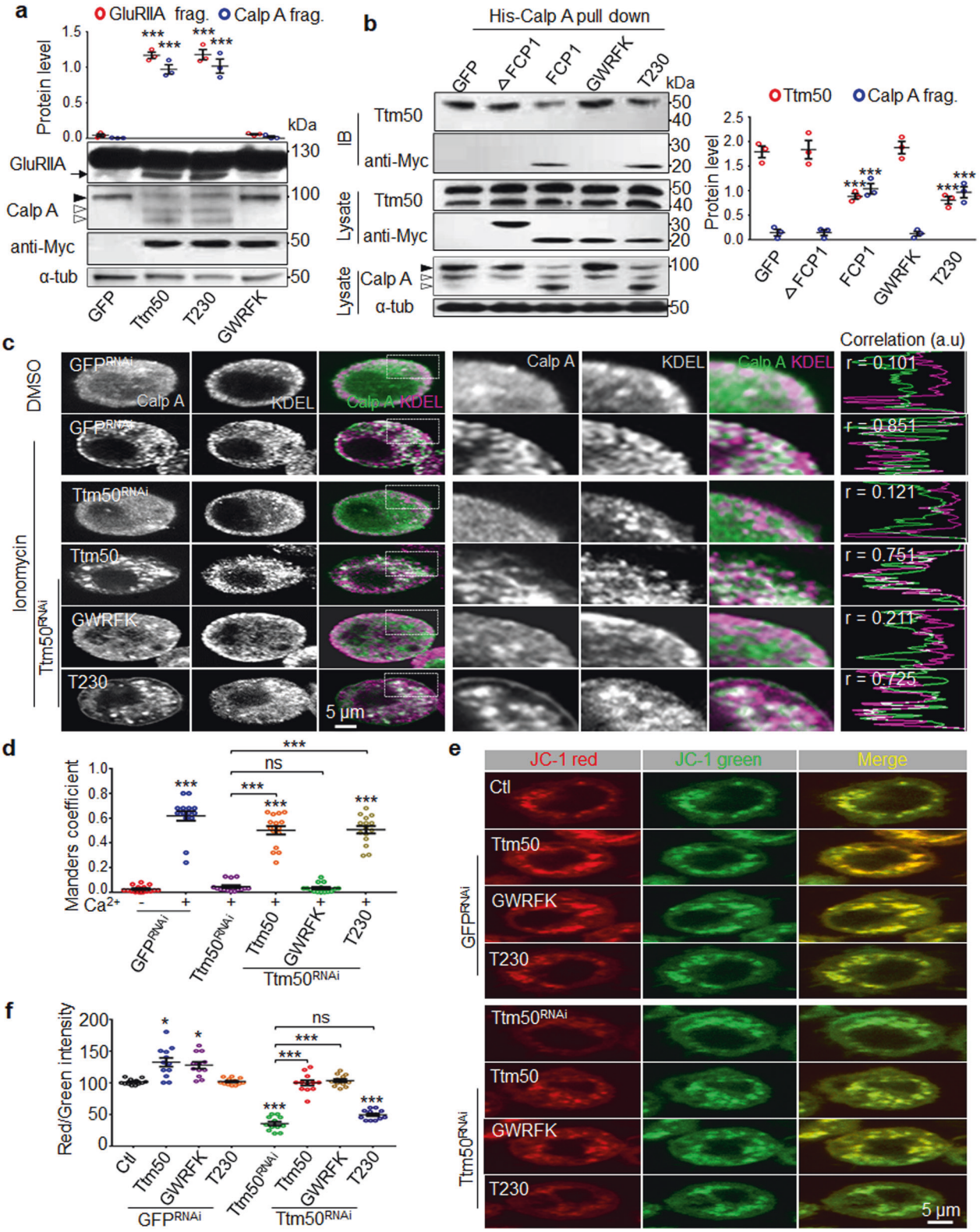

Furthermore, we investigated the binding affinity between Ttm50 and calpain A using bilayer interferometry (BLI) and NTA biosensor kinetic assays. GST-calpain A bound to immobilized His-Ttm50 and His-FCP1, but not His-tagged FCP1-deleted Ttm50 (Fig. 5e–g). Binding between GST-calpain A and Ttm50 was specific since GST alone did not bind His-Ttm50 (Fig. 5h).

Ttm50 and basal calcium levels are required for calpain localization

It has been proposed that calpain activity can be regulated by its subcellular localization,[33] but direct in vivo evidence supporting this is lacking. Herein, we demonstrated that calpain and Ttm50 localize to GM130-positive Golgi and KDEL-positive ER by

Fig. 4 Disruption of the Ttm50–calpain interaction inhibits calpain activity and localization in S2 cells. a Co-expressing Flag-GluRIIA and Myc-tagged wild-type or T230A mutant Ttm50, but not Ttm50 carrying GWRFK-AAAAA mutations in S2 cells increases calpain activity in the presence of 1 mM calcium. Black arrow indicates the fragment of GluRIIA while the arrowheads indicate full-length calpain (black) and autolytic bands (open). Scatter plot graph shows relative levels of GluRIIA and Calp A fragments upon expression of different Ttm50 mutants. $n = 3$, $^{***}P < 0.001$ by one-way ANOVA with Tukey's post hoc test. Data are presented as means ± SEM. **b** S2 cell lysates expressing Myc-tagged FCP1-deleted Ttm50, FCP1, FCP1 harboring GWRFK-AAAAA mutations, and FCP1 carrying T230A mutation were pulled down by *E. coli*-derived His-calp A immobilized on Ni-NTA resin, and the resulting protein complexes were subjected to immunoblotting with the indicated antibodies. S2 cell lysates were also subjected to calcium treatment (1 mM for 30 min) followed by western blotting with anti-Calp A. Scatter plot graph shows relative levels of Calp A fragments and immunoprecipitated Ttm50 upon expression of different Ttm50 mutants. $n = 3$, $^{***}P < 0.001$ by one-way ANOVA with Tukey's post hoc test. Data are presented as means ± SEM. **c** The effect of endogenous Ttm50 and Ttm50 variants on calpain localization to ER in S2 cells. S2 cells treated with ionomycin at 5 μM were co-stained with anti-calp A (green) and anti-KDEL (magenta) antibodies. Pearson correlation coefficient (*r*) is indicated. Scale bar, 5 μm. **d** Manders coefficient of co-localization of endogenous Calp A and KDEL-positive ER in S2 cells. $n = 12$ cells for different treatments, ns, no significance, $^{***}P < 0.001$ by one-way ANOVA with Tukey's post hoc test and student's *t*-test. Data are presented as means ± SEM. **e** Ttm50 regulates MMP in S2 cells. S2 cells were transfected with plasmids expressing the indicated variants of Ttm50 and stained with JC-1. Scale bar, 5 μm. **f** Measurement of the JC-1 intensity ratio. Red staining indicates hyperpolarized mitochondria, while green staining indicates depolarized mitochondria. $n = 10$ cells for each construct, ns, no significance, $^{*}P < 0.05$ and $^{***}P < 0.001$ by one-way ANOVA with Tukey's post hoc test and student's *t*-test. Data are presented as means ± SEM.

immunostaining and fractionation (Fig. 2). We hypothesized that Ttm50 might promote calpain activity by localizing calpain at calcium stores, Golgi and ER. As shown in Fig. 6a, few calpain A puncta were co-localized with Golgi in muscles expressing reduced levels of Ttm50 following RNAi knockdown (Fig. 6a). Quantitatively, the number of calpain A-positive puncta co-localized with Golgi and the degree of overlap were significantly reduced in Ttm50 knockdown muscles compared with controls (Fig. 6c, d). Previous studies showed that Ca-α1D, a L-type voltage-gated calcium channel that facilitates calcium influx across the plasma membrane, is required for calpain activity in dendrite pruning of sensory neurons[9] and downregulation of GluRIIA at NMJ synapses.[10] We therefore examined the calcium requirement for calpain A localization at Golgi, and found that such localization was indeed significantly decreased in Ca-αID knockdown muscle cells (Fig. 6a, c, d). Importantly, reduced calpain A localization to Golgi caused by Ca-αID but not Ttm50 knockdown was restored when muscle cells were treated with calcium at 10 mM for 30 min (Fig. 6a–d). These results demonstrated that both Ttm50 and resting-state levels of calcium are required for normal localization of calpain A to calcium stores Golgi.

Human Tim50 promotes the activity of calpain 1 and 2 in human cells

To determine if the enhancement of *Drosophila* calpain activity by Ttm50 shown above is conserved in mammals, we tested the effect of mitochondrial isoform of Tim50, the human homolog of *Drosophila* Ttm50, on calpain activity using the cleavage of a well-characterized calpain substrate p35 as a readout.[5] As expected, mammalian calpains cleaved p35 to 25 kDa fragments, but this action was abolished by calpeptin, a specific calpain inhibitor (Fig. 7a, b). In vitro experiments showed that the FCP1 domain of human Tim50 effectively enhanced conversion of p35 to p25 by calpains 1 and 2 in a calcium-dependent manner (Fig. 7a–c). Consistently, we observed increased calpain autolysis following FCP1 addition evidenced by an apparent reduction of the full-length calpain 1, though no large autolytic fragments were detected, as the antibody we used recognizes the N-terminal residues 8–33 of calpain 1 (Fig. 7a). As expected, the 43 kDa autolytic fragment of calpain 2 detected by an antibody against the C-terminal domains III and IV of calpain 2 was enhanced when FCP1 was present (Fig. 7b). Furthermore, we found that the human FCP1 domain regulated the reaction velocity of calpains in a calcium- and time-dependent manner. As shown in Supplementary information, Fig. S7a, Ca^{2+} concentrations needed for calpains to reach ½ maximum velocity (*V*max) were ~70 μM for calpain 1, ~5 mM for calpain 2, and ~12 mM for calpain A. When the FCP1 domain was present, calpain activity was significantly increased, and Ca^{2+} concentrations needed for ½ *V*max became ~20 μM for calpain 1, ~1 mM for calpain 2, and ~6 mM for calpain A (Supplementary information, Fig. S7a). In addition to increased calpain sensitivity to calcium, the time required to reach ½ *V*max was reduced by about half following FCP1 addition (Supplementary information, Fig. S7b). Notably, the *Drosophila* calpain A has a similar calcium sensitivity with mammalian calpain 2 (Supplementary information, Fig. S7a, b), in agreement with a previous report.[36] Thus, as with *Drosophila* FCP1 (Fig. 5), the human FCP1 domain also increased mammalian calpain sensitivity to calcium by roughly an order of magnitude.

To validate the regulation of mammalian calpain activity by Tim50, we first performed fractionation experiments from human cell lysates. As shown in Supplementary information, Fig. S7c, d, the level of human Tim50 was several-fold higher in the mitochondrial fraction (Mito) than in non-mitochondrial organelles such as Golgi and ER, and the partitioning of both calpains in mitochondria and Golgi/ER fractions appeared to be similar (Supplementary information, Fig. S7c, d). Unlike two isoforms of *Drosophila* Ttm50, a single 40 kDa Tim50 isoform was detected by a rabbit polyclonal antibody targeting the C-terminal residues 167–249 of Tim50. We speculated that human Tim50 protein was not cleaved into a smaller fragment in the mitochondrial fraction. To verify this possibility, we expressed N-terminal Myc-tagged Tim50 in human cells. As with endogenous Tim50, the same sized 40 kDa Myc-Tim50 was detected in both mitochondria and non-mitochondrial organelles by anti-Myc antibody (Supplementary information, Fig. S7e), consistent with a previous report that human Tim50 is not cleaved at the N-terminus following import into mitochondria.[37]

We then investigated the interaction between Tim50 and calpains by Co-IP in human HEK293 cells (Fig. 7d). Both calpains were detected to be immunoprecipitated by Tim50, but not by control IgGs (Fig. 7d). To further explore the role of Tim50 in regulating calpain activity in human cells, HEK293 cells were transfected with independent Tim50 siRNAs. Results show that Tim50 siRNAs but not scrambled control siRNA suppressed endogenous expression of Tim50, and inhibited the production of p25 from overexpressed p35 (Fig. 7e; Supplementary information, Fig. S7f) and calpain autolysis upon calcium treatment (Fig. 7e). Conversely, overexpression of the mitochondrial isoform of wild-type Tim50 or T149A mutant but not Tim50 mutant carrying the quintuple mutations of the conserved GWRFK motif increased the production of p25 from p35 and calpain autolysis (Fig. 7f). Furthermore, overexpression of wild-type Tim50 or T149A mutant but not Tim50 carrying GWRFK mutations was able to rescue Tim50 siRNA-induced activity inhibition of calpain (Fig. 7f). Taken together, the results show

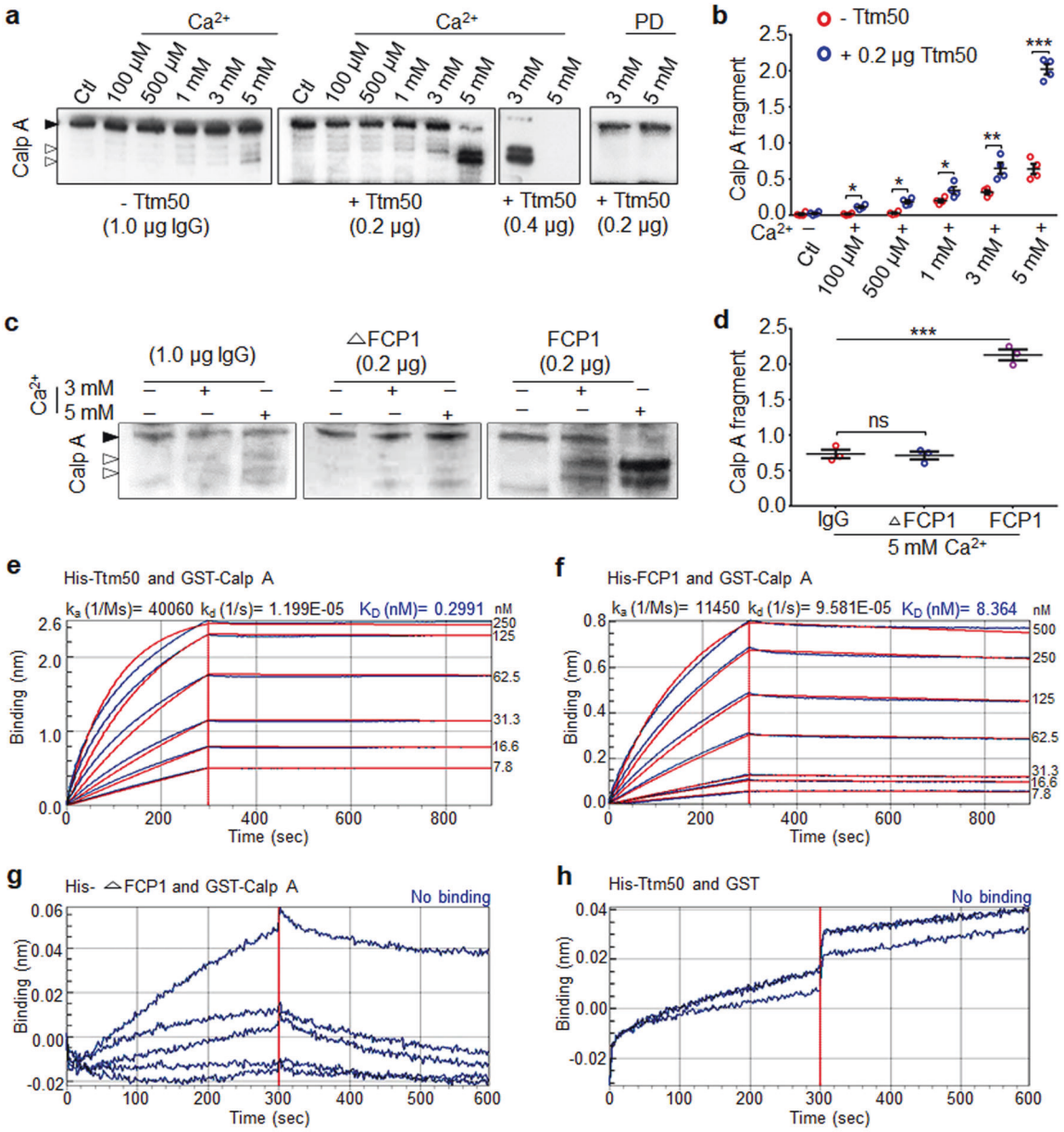

Fig. 5 Ttm50 increases calpain A sensitivity to calcium in vitro. a–c Ttm50 facilitates calpain proteolytic activity via the FCP1 domain in vitro. Purified Ttm50 from *E. coli* were incubated with immunoprecipitated calpain A (0.1 μg) from S2 cells at the indicated calcium concentrations. Calpain autolysis was facilitated by Ttm50 and inhibited by PD150606 (**a**). Relative levels of Calp A fragments in the presence of Ttm50 and different concentrations of calcium (**b**). $n = 4$, $^{*}P < 0.01$, $^{**}P < 0.01$ and $^{***}P < 0.001$ by student's *t*-test. Data are presented as means ± SEM. FCP1-deleted Ttm50 and FCP1 purified from *E. coli* were incubated with immunoprecipitated calpain A at indicated calcium concentrations (**c**). Black arrowheads indicate full-length calpains while open arrowheads indicate autolyzed calpain fragments in **a** and **c**. **d** Quantitative analysis of the density of Calp A fragments in the presence of FCP1-deleted Ttm50 and FCP1. $n = 3$, ns, no significance, $^{***}P < 0.001$ by by student's *t*-test. Data are presented as means ± SEM. **e–h** Ttm50 binds calpain in vitro with high affinity indicated by BLI. Binding of GST-Calp A (**e–g**) and GST alone (**h**) to His-Tim50 (**e**, **h**), His-FCP1 (**f**), and His-ΔFCP1 (**g**) immobilized on Ni-NTA. Association rate (K_a), dissociation rate (K_d), and equilibrium dissociation constant (K_D) were presented.

that facilitation of calpain activity by Ttm50 is conserved in both fruit flies and humans.

DISCUSSION

The main challenge regarding calpain activation is reconciling the high levels of calcium required for activity in vitro with the low calcium levels present in vivo. Although in specific cellular locations calcium levels may be higher than the average in the overall cytoplasm,[13] intracellular calcium alone is probably unable to ensure calpain activation in normal physiological and developmental processes. In the present study, we show that Ttm50 acts as a calpain anchor and activator, as presented in Fig. 6e. Interaction with Ttm50 facilitates calpain activity by localizing calpain to calcium stores, while simultaneously increasing the calcium sensitivity of the enzyme.

Ttm50 anchors calpain at Golgi/ER

The subcellular localization of calpains varies greatly. For example, mammalian calpains are diffusely distributed in the cytoplasm with enrichment at the ER, Golgi or plasma membrane, depending on specific calpains and cell types.[38]

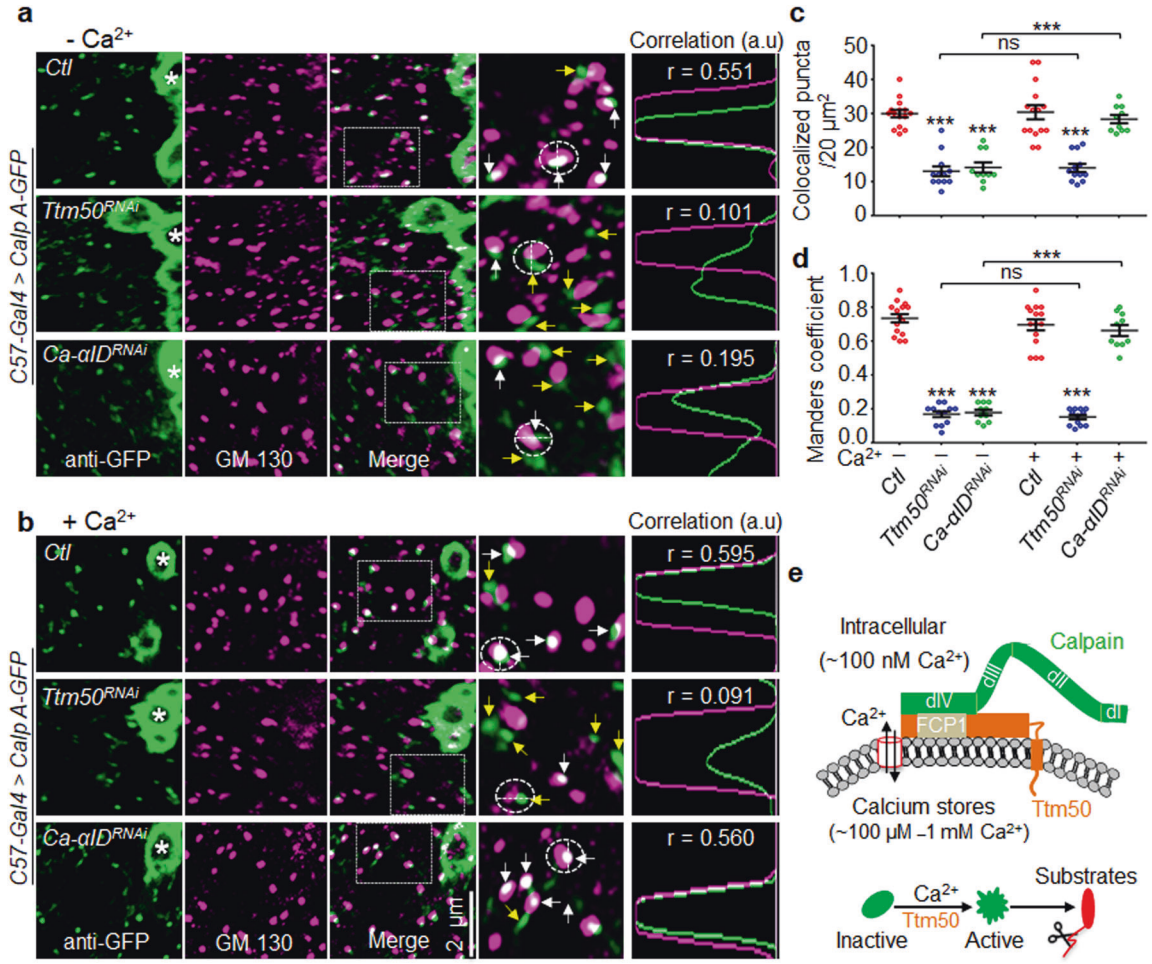

Fig. 6 Ttm50 and basal levels of calcium are required for calpain localization at Golgi. a, **b** Calpain localization at Golgi is dependent on Ttm50 and calcium. Representative images are shown for cytoplasmic areas near NMJ4 synapses (white asterisks) of different genotypes co-stained with anti-GFP (green) and Golgi marker anti-GM130 (magenta) antibodies (**a**). In **b**, dissected muscles were treated with calcium at 10 mM for 30 min. White arrows indicate puncta positive for both calpain and Golgi, while yellow arrows indicate puncta positive only for calpain. Scale bar, 2 μm. Pearson correlation coefficient (*r*) is indicated. **c**, **d** Quantitative analysis of the number of puncta containing both calpain and Golgi per 20 μm^2 muscle area (**c**) and Manders coefficient (**d**) for different genotypes with or without calcium treatment. $n = 15$, 12, and 10 muscle cells for wild type, *Ttm50-RNAi* and *Ca-α1D-RNAi*, respectively, ns, no significance, $^{***}P < 0.001$ by one-way ANOVA and student's *t*-test. Data are presented as means ± SEM. **e** Working model of calpain activation facilitated by Ttm50. Ttm50 is an integral membrane protein that recruits calpains via FCP1 to Golgi/ER.

The phosphoinositol PIP2 is required for localization and subsequent activation of calpain 2 at the plasma membrane of cultured cells.[33] However, phospholipids are common activators of many enzymes, and hence cannot serve as specific calpain activators.[3] Thus, the mechanisms responsible for calpain localization at membrane organelles remain unclear. Herein, we report that the integral membrane protein Ttm50 mediates calpain localization at calcium stores Golgi and ER and thereby enhances activation through the locally high calcium concentrations present therein. Knockdown of Ttm50 disrupts the calcium-dependent mobilization of calpain A to Golgi and ER (Figs. 4 and 6). Furthermore, the interaction between Ttm50 and calpain was enhanced by calcium, and localization of calpain A at Golgi was dependent on calcium (Figs. 3 and 6). Thus, calcium-dependent calpain localization at Golgi/ER via Ttm50 provides a possible explanation for in vivo activation of calpains. We note that Ttm50 and calpain only localize to a subset of Golgi/ER and part of Golgi/ER (Figs. 2 and 6). So far, we do not have a satisfactory answer for the specificity of localization. It is possible that Golgi/ER population, as well as the structure of individual Golgi/ER in a cell is not homogenous.

Ttm50 increases the calcium sensitivity of calpain

The mechanism by which the proteolytic activity of calpain is regulated in vivo is currently unclear. Genetic and optogenetic studies showed that an influx of calcium to the cytoplasm from extracellular space activates calpains.[9,10] In the present study, we show that calcium release from calcium stores is sufficient for calpain activation. Specifically, 10 μM of thapsigargin (Tg) induced a mild but significant downregulation of GluRIIA via calpains, while treatment with 10 μM ionomycin in Ca^{2+}-free medium decreased GluRIIA levels to a greater extent at NMJ synapses (Supplementary information, Fig. S8), suggesting that fast depletion of calcium from Golgi/ER is sufficient to activate calpains. The different results from Tg treatment and ionomycin treatment in Ca^{2+}-free medium are probably due to the fact that ionomycin is an ionophore that causes faster and more complete emptying of Golgi/ER calcium stores than Tg. Moreover, we characterized Ttm50, the first in vivo activator of calpain discovered to date. Ttm50 physically interacts with calpain via the C-terminal FCP1 domain. Furthermore, Ttm50 interacts with calpain in a calcium-dependent manner, and the interaction with Ttm50 increases the calcium sensitivity of calpain by roughly an order of magnitude. More specifically, the FCP1

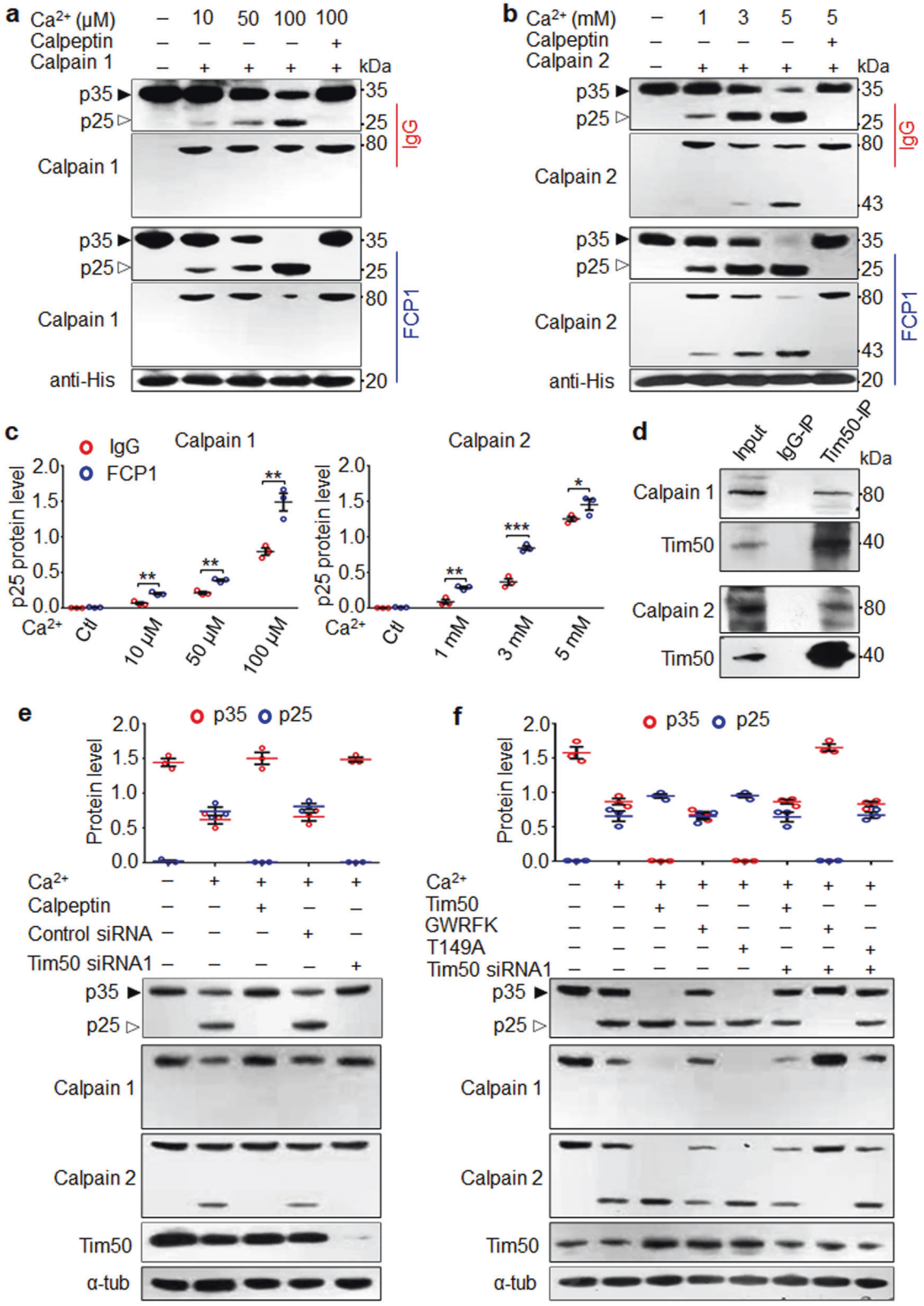

domain of Ttm50 and Tim50 is sufficient to enhance calpain activity by in vitro assays (Fig. 7a–c; Supplementary information, Fig. S7a, b).

Calcium-binding sites are conserved in calpains from *Drosophila* to humans.[39,40] However, different members of the calpain family exhibit differences in sensitivity to calcium. The present study reveals an unexpected mechanism by which Ttm50 facilitates calpain activity. Knockdown of Ttm50 results in inhibition of calcium-induced calpain proteolytic activity in vivo and in cultured cells. Conversely, the level of calpain autolysis and the efficiency with which calpain cleaves the p35 substrate are increased significantly as a result of direct protein–protein interaction with

Fig. 7 Human Tim50 promotes calpain 1 and 2 activity in human cells. a, **b** The FCP1 domain of human Tim50 increases calpain-mediated cleavage of p35 to p25 in vitro. The p35 protein from human cells was subjected to Co-IP and incubated with calpain 1 (**a**) and calpain 2 (**b**) (0.2 μg for each calpain) in the presence of different calcium concentrations with or without human FCP1 (0.5 μg). **c** Quantitative analysis of the p25 protein in the presence of different concentrations of calcium. $n = 3$, $^{*}P < 0.05$, $^{**}P < 0.01$ and $^{***}P < 0.001$ by student's *t*-test. Data are presented as means ± SEM. See also Supplementary information, Fig. S7 for the effect of the FCP1 domain of *Drosophila* Ttm50 on *V*max for calpain activity in vitro. **d** Western blot analysis showing that Tim50 effectively immunoprecipitated calpains from HEK293 cells. See also Supplementary information, Fig. S7 for Tim50 and calpain localization at different cellular fractionations. **e** Tim50 is required for calpain activity in HEK293 cells. HEK293 cell lysates were treated with calcium at 3 mM for 30 min followed by immunoblotting with indicated antibodies. **f** The GWRFK motif of Tim50 is required for calpain activity in HEK293 cells. Plasmids expressing wild-type or mutated Tim50 (GWRFK-AAAAA and T149A mutant) were transfected into HEK293 cells alone or co-transfected with Tim50 siRNA. HEK293 cell lysates were treated with calcium at 3 mM for 30 min followed by immunoblotting with indicated antibodies. In **e** and **f**, scatter plot graphs show relative protein levels of p35 and p25 upon different treatments. $n = 3$.

Ttm50 in cultured cells and in vitro (Fig. 7). We suspect that Ttm50 binding may increase the calcium sensitivity of calpain by changing the conformation of the enzyme so that the calcium-binding domains are exposed and become accessible to calcium. Alternatively, this may increase the affinity for calcium. It is also possible that both mechanisms may operate simultaneously.

Ttm50 enhances calpain activation independent of its mitochondrial function

Ttm50 is a *Drosophila* homolog of human Tim50, a subunit of the Tim23 complex involved in the import of proteins across the mitochondrial inner membrane into the matrix.[20,23,34] In the present study, we found that in addition to mitochondrial localization as reported for *Drosophila* Ttm50, Ttm50 was also localized at Golgi and ER in muscles and S2 cells (Fig. 2; Supplementary information, Fig. S4i, j). While cell lysate fractionation analysis of S2 cells revealed substantial localization of Ttm50 in mitochondria (Fig. 2), we observed rare mitochondrial localization of Ttm50 by co-staining with MitoTracker in muscle cells (Fig. 2). The co-staining results contradict the reported mitochondrial localization in fat body cells,[23] suggesting a possible cell type-specific localization, or another possibility that the epitope recognized by anti-Ttm50 might be embedded in the Tmi23 complex, or both. In any case, our study uncovers a crucial role for Ttm50 but not other subunits of the Tim23 complex (data not shown) in regulating calpain localization and activation via the FCP1 domain, as demonstrated by in vivo and in vitro analyses. This reveals a novel function of Ttm50 that is independent of the Tim23 complex. Exactly how the independent functions of Ttm50 as a calpain anchor/activator and a subunit of Tim23 translocase are balanced and precisely regulated remains to be further investigated.

Missense mutations R217W and T252M of human Tim50 are associated with intellectual disability and epilepsy.[32] Other studies showed that Tim50/Ttm50 is essential for cell growth in yeast and *Drosophila*.[20,23] It would be intriguing to examine if reduced calpain activity, defective mitochondrial function, or both contribute to Tim50/Ttm50 mutant phenotypes in different organisms. While we show in the present study that *Drosophila* Ttm50 is expressed in both mitochondria and Golgi/ER, its function has so far only been analyzed in mitochondria in various organisms.[20,23,37] In support of the conserved Ttm50–calpain interaction from *Drosophila* to mammals, human Tim50 is both required and sufficient for human calpain activation (Fig. 7). Our finding that Ttm50 is a calpain anchor and activator is consistent with a previous report that only one-third of Tim50 molecules were shown to stably associate with the Tim23 complex in mitochondria, while the rest formed a pool that remains distinct from the Tim23 complex.[20]

Calpains function downstream of physiological calcium transients in vivo

Calpain activation is triggered by abnormally high calcium levels associated with pathologies, such as ischemic insults and neurodegeneration,[6,41] but the in vivo role of calpain under physiological conditions is largely unknown. Calcium signaling occurs in different subcellular compartments with spatiotemporal precision.[13] For example, specific processes such as muscle contraction, neuronal excitation and stress lead to an increase in calcium influx in a spatial manner.[12,13] Interestingly, genetic and optogenetic manipulation of calcium influx at sensory neurons[9] and NMJ synapses[10] revealed that calpains function downstream of calcium influx during normal development. It is speculated that controlled and localized calpain activation is accomplished by an intrinsic property of neurons that is, by an increase in excitability of specific dendritic branches to induce local calcium transits.[9] As axonal and dendritic pruning is a fundamental process in brain development and disease progression, and localized changes in dendritic branch excitability are observed in different types of mammalian neurons,[42,43] it is intriguing to speculate that enhanced activation of calpains by Ttm50 is likely involved in the process of neuronal remodeling.

Most previous studies in recent decades have focused on the pathological role of calpains in injuries and pathologies, while regulation of calpain activity in normal physiology and development has been largely ignored. Our current results reveal that Ttm50 facilitates calpain activation by two distinct mechanisms: mediating calpain localization at Golgi/ER, and increasing the sensitivity of calpains to calcium. In addition, the high concentrations of calcium at local compartments such as calcium stores may further enhance the protein–protein interaction between Ttm50 and calpain. In summary, our findings offer novel insight into the mechanism by which calpain activity is precisely regulated at both molecular and cellular levels. This novel mechanism suggests potential targets for drug development against calpain-related disorders.

MATERIALS AND METHODS

Drosophila stocks

All fly stocks were reared on standard cornmeal food at 25 °C. All flies were obtained from Bloomington *Drosophila* Stock Center (http://flystocks.bio.indiana.edu) or Tsinghua University *Drosophila* Stock Center (http://fly.redbux.cn/) unless otherwise noted. The w^{1118} strain was used as the wild-type control in all experiments. *UAS-Calp A* lines were described.[10] *UAS-calpain A-GFP* flies were generously provided by Dr. H. Araujo at the Federal University of Rio de Janeiro.[44] *UAS-Ttm50-HA* flies were supplied by Dr. S. Sugiyama at Nagoya University, Japan.[23] All *Drosophila* stocks are listed in Supplementary information, Table S1.

Immunohistochemistry

Immunocytochemistry was performed as described previously with minor modifications.[10] Third instar larvae were dissected in ice-cold calcium-free HL3 saline (70 mM NaCl, 5 mM KCl, 20 mM $MgCl_2$, 10 mM $NaHCO_3$, 5 mM trehalose, 5 mM HEPES, 115 mM sucrose; pH 7.3), and then fixed in either 100% methanol on ice for 10 min (for anti-GluRIIA and anti-Ttm50) or 4% paraformaldehyde for 30 min (for all other antibodies), followed by washing with 0.2% Triton X-100 in phosphate buffered saline. The following

primary antibodies were used: mouse anti-GluRIIA (1:500, 8B4D2, Developmental Studies Hybridoma Bank, RRID:AB_528269), rabbit anti-calp A (1:500, Institute of Enzymology, Biological Research Center, Hungarian Academy of Science, RRID:AB_2569845), mouse anti-HA (1:100, Sigma, RRID:AB_514505), mouse anti-Myc (1:100, Milipore, RRID:AB_309938), mouse anti-Flag (1:100, Sigma, RRID:AB_259529), rabbit anti-GM130 (1:100, Abcam, RRID:AB_732675), mouse anti-GM130 (1:100, Santa Cruz, sc-55591), rat anti-KDEL (1:100, Abcam, RRID:AB_880636), and mouse anti-GFP (1:300, Snata Cruz, RRID:AB_627695). Alexa 649-conjugated anti-horseradish peroxidase (anti-HRP, 1:100, Jackson Immuno Research, RRID:AB_2340866), Alexa 488- or 568-conjugated anti-mouse, anti-rabbit and anti-rat secondary antibodies (Invitrogen, RRID:AB_2633275 and RRID:AB_141371) were used at 1:500. All antibodies are listed in Supplementary information, Table S2. MitoTracker deep red FM, a mitochondrial marker (Invitrogen, Cat# M22426) was used at 20 μM. To-PRO-3 Iodide, a nuclear stain (Invitrogen, Cat# T3605) was used at 1:700.

Measurement of calcium in larval muscles and live S2 cells was performed as described previously.[45] Rhod-2AM stain (Invitrogen, MP01244), a calcium indicator for mitochondria, was used at 200 nM. Fluo-4AM (Invitrogen, MP01240), an indicator for cytoplasmic calcium, was used at 5 μM. Larval muscles or S2 cells were incubated with the calcium stains for 30 min at 37 °C, After staining, the cells were washed in calcium-free HL.3 saline containing 2 mM EGTA to remove non-specific staining. 10 μM ionomycin (Sigma, Cat# I9657) was used to stimulate calcium release from intracellular organelles.

Measurement of MMP in S2 cells was performed largely following a previous protocol using JC-1 stain (Invitrogen, T3168).[35] JC-1 stain is a cationic dye that exhibits potential-dependent accumulation in mitochondria, indicated by a fluorescence emission shift from green (~525 nm) to red (~590 nm). We used oligomycin at 1.0 μg/mL and FCCP at 2 μM to monitor MMP in S2 cells. S2 cells were incubated with the JC-1 stain for 15 min at 37 °C. After washing, JC-1 staining was visualized directly under a confocal microscope. These reagents are listed in Supplementary information, Table S3.

Generation of a rabbit antibody against Ttm50

Polyclonal antibody against Ttm50 was raised by immunizing rabbits with peptides containing amino acids 81–97 and 207–223 of *Drosophila* Ttm50 (accession No. NP_570027). The antibody was used at 1:1000 for both staining and western blotting.

Construction of HA-tagged Ttm50 flies

We knocked in a 3× HA tag before the stop codon of the endogenous *Ttm50* according to previously published homology-directed repair procedures[46] at Fungene Biotech (http://www.fgbiotech.com). The knockin sequence is attatgggccgcatctttTACCCATACGATGTTCCTGACTATGCGggcTATCCCTATGACGTCCCGGACTATGCAggatccTATCCATATGACGTTCCAGATTACGCTgctcagagcggtatgcagTAG. The capital letters represent HA-coding sequence while lowercases represent linkers. TAG is the stop codon.

Dendrite imaging and quantification

Individual animals were collected at pupariation and maintained at 25 °C in a Petri dish with moist filter paper. Staging was determined as hours after puparium formation (APF). For whole-mount live dendrite imaging, pupae were mounted in glycerol (50%) under coverslips. Dendrites of class IV dendritic arborization (da) sensory neurons expressing mCD8-GFP under the control of *ppk-Gal4* were visualized directly under a confocal microscope as previously described.[9,47]

Immunoprecipitation and immunoblotting

Western blotting was performed as described previously.[10,48] Third instar larvae muscles were homogenized in ice-cold RIPA lysis buffer (50 mM Tris-HCl at pH 7.4, 150 mM NaCl, 0.1% SDS, 1% NP-40) containing 1× protease inhibitors (Set 1, Roche). The lysates were centrifuged at 18,000× *g* for 10 min and then resulting supernatant was used for western blotting with the following primary antibodies: mouse anti-GluRIIA (1:1000), rabbit anti-calp A and anti-calp B (1:1000), mouse anti-α-tubulin (1:50,000, Millipore, RRID:AB_2617116), and anti-GFP (1:700). The secondary antibody was HRP-conjugated anti-mouse IgG (Sigma, RRID:AB_258431) or anti-rabbit IgG (Sigma, RRID:AB_257896) used at 1:50,000. Protein bands were visualized using a chemiluminescent HRP substrate (Millipore). For immunoprecipitation (IP), larval muscle lysates were incubated with appropriate antibodies (2 μg antibody). The protein–antibody complexes were then precipitated with protein A or protein G-conjugated Dynabeads (Thermo Scientific, Cat# 10006D for protein A and Cat# 10003D for protein G) for further analysis.

Isolation of subcellular organelles by optiprep velocity gradients and differential centrifugation

The subcellular fractionation from S2 cells was performed as described previously.[24,26] Briefly, five 10-cm plates of S2 cells were washed with ice-cold PBS with 1 mM PMSF. Cells were then homogenized in 5 mL of buffer A (0.3 M sucrose, 1 mM EDTA, 1 mM $MgSO_4$, 10 mM MES-KOH, pH 6.5) containing 1 mM PMSF by nitrogen cavitation bomb for 10 min at 450 pounds per Square Inch Pressure (psi). The cell homogenates were centrifuged at 1000× *g* for 5 min to remove debris. The post-nuclear supernatant was collected and loaded on top of a discontinuous Optiprep™ density gradient medium (Sigma, Cat# MFCD00867965) composed of 5 layers (30%, 23.4%, 17.6%, 13.2%, and 8.8%). 30% OptiPrep medium was prepared as a stock in buffer B (2 mM EGTA, 20 mM MES-KOH, pH 6.5), and the rest gradients were made by diluting 30% OptiPrep medium with buffer A containing 1 mM PMSF in a swinging-bucket centrifuge (SW40) tube, and the sample was centrifuged at 100,000× *g* for 80 min. Based on visible appearance, 5 fractions were collected and washed 3 times in buffer A. Then, the fractions were centrifuged at 20,000× *g* for 15 min. The supernatant was discarded, and the resulted pellets were processed for western blotting. Equal amounts of proteins for each fraction were subjected to western blot analysis with antibodies against various organelle markers including rabbit anti-cytochrome oxidase subunit IV (CoIV) (1:2000, from Dr. Tao Wang at National Institute of Biological Sciences (NIBS), China), rabbit anti-GM130 (1:1000), and rabbit ribophorine II (1:500, NOVUS, AB_2254079).

For differential centrifugation, muscles or S2 cells were harvested and washed in ice-cold PBS. The cells were broken by multiple shifting the cells from 37 °C to liquid nitrogen for 5 times 5 min each.[25] The cell homogenates were first centrifuged at relatively low speeds at 1000× *g* for 10 min to remove unbroken cells and nuclei. The supernatant was next centrifuged at a higher speed of 8000× *g* or 35,000× *g* for 30 min, which sediments the mitochondria. A subsequent ultracentrifugation (150,000× *g* for 120 min, Optima MAX.XP) resulted in enrichment of Golgi and ER. Equal amounts of proteins for each fraction were processed for western blotting.

Prediction and verification of MTS cleavage sites in Ttm50

Mitofates (http://mitf.cbrc.jp/MitoFates/cgi-bin/top.cgi/)[28] and TargetP (http://www.cbs.dtu.dk/services/TargetP/)[29] were used to identify putative MTS cleavage sites in the N-terminal of Ttm50. Two high score MTS cleavage sites at RGY and KQE were predicted by Mitofates and TargetP. For site-directed mutagenesis, the predicted cleavage sites were mutated with the KOD-Plus-Mutagenesis kits (KOD-201, F0934K, China) according to the manufacturer's recommendations. The following primers were used to mutate the predicted sites to alanine. For KQE-AAA mutation, we used forward primer

(5′-CACAGCGGCTGCCGCCAGCAGCACAACCGCGGCGGCAGCTGGAGCC-3′) and reverse primer (5′-GGCTCCAGCTGCCGCCGCGGTTGTGCTGCTGGCGGCAGCCGCTGTG-3′). For RGY-AAA mutation, we used forward primer (5′-CTGCACACAGCGGCTGCCGCCAGCAGCACAACC-3′) and reverse primer (5′-GGTTGTGCTGCTGGCGGCAGCCGCTGTGTGCAG-3′). For R80-A mutation, we used forward primer (5′-ATCCTGCACACAGCGGCTGGCTACAGCAGCACA-3′) and reverse primer (5′-TGTGCTGCTGTAGCCAGCCGCTGTGTGCAGGAT-3′). For KQE-AAA mutation, the forward primer (5′-GCAGCACAACCGCGGCGGCAGCTGGAGCCACTGGC-3′) and reverse primer (5′-GCCAGTGGCTCCAGCTGCCGCCGCGGTTGTGCTGC-3′) were used. Ttm50^{N200}-GFP with or without mutations expressed in S2 cells was fractionated and tested for MTS cleavage by western blot analysis.

Identification of critical residues in FCP1 domain for Ttm50/calpain interaction

For identification of amino acid residues critical for Ttm50/calpain interaction, we generated serial mutations in the 224–295 aa peptide of the FCP1 domain; each mutant contained ten contigous amino acids muated to alanines. Mutations were generated with the KOD-Plus-Mutagenesis kits (KOD-201, F0934K, China). The primers for generating point mutations are listed in Supplementary information, Table S4.

Calcium treatment of larval muscles

To induce activation of the endogenous calpains, larvae were dissected in Ca^{2+}-free HL3 saline. Ca^{2+}-free HL3 saline containing 0.5 mM EGTA was used as unstimulated control. For calcium stimulation, dissected larvae were incubated with HL-3 solution containing 1–10 mM $CaCl_2$ and 10 μM ionomycin[49,50] (Sigma, Cat# I9657) for 30 min and then washed in Ca^{2+}-free HL3 saline and incubated for 10 min. For calpain activity inhibition, the samples were incubated for 30 min in HL3 saline containing 20 μM PD150606[51] (Abcam, Cat# ab141464) prior to the addition of calcium. For immunohistochemistry, differently treated groups were dissected and processed at the same condition.

Cell culture and plasmid construction

Drosophila S2 cells (RRID: CVCL_Z232) were cultured as previously described.[10,52] S2 cells were maintained at 25 °C in optimized serum-free medium (SF-900 II, Gibco). Cultured cells were resuspended in the medium at a final concentration of 1×10^6 cells/mL and plated at 1 mL/well in six-well culture plates. Cells were transfected after 24 h incubation using Cellfectin II reagent (Invitrogen) and expression was induced with 0.5 mM $CuSO_4$ for 48 h. Finally, transfected cells were lysed in RIPA buffer for 1 h at 4 °C. The primers for generating various constructs are listed in Supplementary information, Table S5.

For Co-IP assay, the following fusion proteins were co-expressed in S2 cells: HA-Calp A or His-Calp B with Myc-Ttm50, Flag-tagged calpain A truncations with Myc-tagged Ttm50, and Myc-tagged Ttm50 truncations with Flag-Calpain or Flag-dIV. For IP, the S2 cell lysates were incubated with the following antibodies (2 μg): anti-Flag (1:1000), anti-His (1:1000, Abcam, Cat# ab14923), anti-HA (1:1000), anti-Myc (1:1000), and anti-calpain A (1:1000), followed by precipitation with 50 μL protein A or G-conjugated Dynabeads. An equal amount of rabbit or mouse IgG (2 μg, Sigma) was used as a negative IP control.

RNAi-mediated knockdown of gene expression was performed as described previously.[53] The following primers were used for amplification to generate templates for dsRNA synthesis: 5′-TAATACGACTCACTATAGGGATGAGCATGAGCAATGGCAC-3′ and 5′-TAATACGACTCACTATAGGGAACTCGTAGACGGCCCAGAAT-3′ for *Ttm50* dsRNA1; 5′-TAATACGACTCACTATAGGGCGGCAAGCCCGAGGTGGACC-3′ and 5′-TAATACGACTCACTATAGGGGTCCGGATGCATCTTGGTGGC-3′ for *Ttm50* dsRNA2. For control GFP dsRNA, the primers 5′-TAATACGACTCACTATAGGGATGGTGAGCAAGGGCGAGG-3′ and 5′-TAATACGACTCACTATAGGGGTGCCCCAGGATGTTGCCGTC-3′ were used. The PCR products were used as templates for synthesis of dsRNA using the MEGAscript T7 kit (Ambion). 10 μg dsRNA was added to S2 cells after culturing for 24 h.

Human HEK293 cells were cultured in Dulbecco's modified Eagle's medium supplemented with 10% fetal bovine serum (Invitrogen) at 37 °C in a humidified incubator with 5% CO_2 as previously described.[52] siRNAs for knockdown of human Tim50 were purchased from Santa Cruz (sc-63130 and sc-63129) and a non-targeting 20–25 nt siRNA (sc-37007) designed as a negative control were transfected into HEK293 cells using X-tremeGENE^{TM} siRNA transfection reagent (Roche). Double-stranded (ds) RNAs for RNAi are listed in Supplementary information, Table S6. p35 and Tim50 cDNAs were obtained with reverse transcription-PCR using total RNA from HEK293 cells as a template and subcloned into pCS2 and pCDNA3, respectively. Antibodies used in western blotting, Co-IP, fractionation and activity experiments were mouse anti-calpain 2 (1:1000, Sigma-Aldrich Cat# C268, RRID:AB_258813), mouse anti-calpain 1 (1:200, Santa Cruz Biotechnology, Cat# sc-271313, RRID: AB_10610038), rabbit anti-Tim50 (1:500, Abcam, Cat# ab204486), mouse anti-p35 (1:500, Santa Cruz Biotechnology, Cat# sc-293184), mouse anti-Tom20 (1:1000, Santa Cruez, Cat# sc-17764), and rabbit anti-mannosidase (1:1000, Abcam, Cat# ab12277). For the in vitro experiments, calpain 1 purified from human erythrocytes (Cat# 208713), recombinant rat calpain-2 purified from *E. coli* (Cat# 208718) and the calpain inhibitor calpeptin (100 μM) (Cat# 208904) were purchased from Merck Milipore.

Protein purification and in vitro binding assay

DNA sequence encoding GST-Calp A was synthesized and cloned into PGEX-4T-1 vector between *Bam*HI and *Eco*RI. His-Calp A, His-Ttm50, His-FCP1 (224–367 aa), and His-tagged FCP1-deleted Ttm50 were synthesized and cloned into pET 28a vector between *Bam*HI and *Xho*I restriction sites. Proteins were expressed in *E. coli* under kanamycin selection. *E. coli* were grown in lysogeny broth (LB) (Sigma, Cat# L7275) at 37 °C, and protein expression was induced with 1 mM isopropyl-β-D-thiogalactopyranoside (IPTG) (Sigma, Cat# 367-93-1) for 4 h at 37 °C. *E. coli* were harvested by centrifugation at 5000× *g* and lysed by ultrasonication in PBS. Exogenous proteins were expressed in the form of inclusion body and harvested by centrifugation at 13,000× *g*. Inclusion body was dissolved in dissolution buffer (8 M urea in PBS, Sigma, Cat# 57-13-6) which contains 30 mM imidazole (Sigma, Cat# 288-32-4). His-tagged proteins were purified by Ni-NTA Resin (Thermo Fisher, Cat# 88221) and eluted in dissolution buffer which contains 300 mM imidazole. Eluted protein was refolded in 6 M, 4 M, 3 M, 2 M, 1 M, and 0 M urea gradient refolding buffer (5% glycerol, 1% arginine, 2% glycine in PBS) by dialysis. GST-Calp A was purified by glutathione sepharose beads (Healthcare, Cat# 17-0756-01). Refolded proteins were concentrated to 1 mg/mL and stored at −80 °C.

For in vitro binding assays, 10 μg GST-Calp A protein (purified from *E. coli*) immobilized on glutathione sepharose beads was incubated with 10 μg of His-tagged fusion proteins in 1 mL of lysis buffer (100 mM HEPES, 300 mM NaCl, 20% glycerol, 10% NP40). After incubation for 12 h at 4 °C with gentle shaking, the beads were washed 3 times in washing buffer (100 mM HEPES, 300 mM NaCl, 20% glycerol, 10% NP40, 2 mM DTT). Conversely, 10 μg of purified His-tagged proteins immobilized on Ni-NTA resin were incubated with GST-Calp A or GST alone in lysis buffer. Then, beads with protein complexes were washed 5 times in 60 mM of the imidazole and eluted in 300 mM of the imidazole. Finally, the bound proteins from both assays were subjected to SDS-PAGE for immunoblotting or Coomassie blue staining.

Biolayer interferometry

The real-time binding affinity of His-tagged Ttm50 or FCP1 to GST-Calp A was monitored using an Octet Red 96 system (ForteBio, https://www.moleculardevices.com/products/biologics/label-free-

bli-detection/8 channel-octet-systems). Association rate (K_a), dissociation rate (K_d), and equilibrium dissociation constant (K_D) were determined based on the 1:1 interaction model. The average binding affinity K_D represents a ratio of K_d/K_a, calculated from binding results for different concentrations. The Octet kinetics buffer contains 10 mM $NaPO_3$, 150 mM NaCl, 0.02% Tween 20, 0.05% sodium azide, and 1 mg/mL BSA (pH 7.4).

Imaging and data analysis

Images were collected using an Olympus Fluoview FV1000 confocal microscope with a 40×/3NA or 60×/3NA oil objective and FV10-ASW software (https://www.olympus-lifescience.com/en/, RRID: SCR_014215) or with a Leica confocal microscope using a 40×/3NA oil objective and LAS AF software (http://www.leica-microsystems.com/, RRID:SCR_013673). The type Ib NMJs of muscle 4 on abdominal segments 2 and 3 of each larva were captured using the same settings for statistical analysis. Immunostaining intensities were quantified using Image J (National Institutes of Health, Bethesda, MD, USA; http://www.lmagej.nih.gov/ij/, RRID: SCR_003070), with anti-HRP staining as an internal control for quantification. An arbitrary threshold was set for each channel and used for all relevant images. The intensity of synaptic GluR signal within the region of interest (ROI) defined by HRP staining was normalized to the average of HRP intensity. To quantify protein levels of target proteins, positive signals on western blots from multiple independent repeats were calculated using ImageJ and normalized to the loading control. An arbitrary (a.u.) unit was used to show the ratio of amount of calpain autolytic fragment density to a predetermined reference measurement by ImageJ. Each experiment was repeated for at least three times. Statistical comparisons were performed using GraphPad prism 6. All data were expressed as means ± standard error of the mean (SEM).

Calpain localization at Golgi/ER was quantified by calculating the number and percentage of calpain and Golgi/ER co-localization puncta in 20 μm^2 using ImageJ. The extent of co-localization was analyzed by Manders coefficients and Pearson correlation coefficient (r) (https://imagej.net/colocalization_Analysis).[54] All the data are expressed as means ± SEM. Multiple group means were evaluated by one-way ANOVA with Tukey's post hoc tests for pairwise comparisons or Student's t-tests when appropriate. All comparisons were between a specific genotype and the control unless otherwise indicated.

ACKNOWLEDGEMENTS

This work was supported by the Strategic Priority Research Program B of the Chinese Academy of Sciences (XDBS1020100) and the National Science Foundation of China (31110103907 and 31490590) to Y.Q.Z. and (31500824) to G.Z. We thank Drs. Endre Kókai and Helena Araujo for antibodies and flies. We thank Bloomington and Tsinghua stock centers for supplying stocks. We are grateful to Dr. Yuanyuan Chen (Institute of Biophysics, CAS, China) for technical help with BLI experiment; Dr. Tao Xu and Ms. Li Min (Institute of Biophysics, CAS, China) for advice and technical assistance with fractionation experiments; Dr. Wenhua Li (Institute of Genetics and Developmental Biology (IGDB), CAS, China) for technical assistance with plasmid construction; Drs. Thomas L. Schwarz, Yuhang Chen, Xun Huang, Tieshan Tang, Yi Shi, and Dangsheng Li for discussion.

AUTHOR CONTRIBUTIONS

E.M., G.Z., and Y.Q.Z. conceived and designed the experiments; E.M., G.Z., and Q.W. performed the experiments; E.M., G.Z., and Y.Q.Z. analyzed the data and wrote the manuscript.

ADDITIONAL INFORMATION

Supplementary information accompanies this paper at https://doi.org/10.1038/s41422-020-0388-4.

Competing interests: The authors declare no competing interests.

REFERENCES

1. Hanna, R. A., Campbell, R. L. & Davies, P. L. Calcium-bound structure of calpain and its mechanism of inhibition by calpastatin. *Nature* **456**, 409–412 (2008).
2. Strobl, S. et al. The crystal structure of calcium-free human m-calpain suggests an electrostatic switch mechanism for activation by calcium. *Proc. Natl. Acad. Sci. USA* **97**, 588–592 (2000).
3. Ono, Y., Saido, T. C. & Sorimachi, H. Calpain research for drug discovery: challenges and potential. *Nat. Rev. Drug Discov.* **15**, 854–876 (2016).
4. Saito, K., Elce, J. S., Hamos, J. E. & Nixon, R. A. Widespread activation of calcium-activated neutral proteinase (calpain) in the brain in Alzheimer disease: a potential molecular basis for neuronal degeneration. *Proc. Natl. Acad. Sci. USA* **90**, 2628–2632 (1993).
5. Lee, M. S. et al. Neurotoxicity induces cleavage of p35 to p25 by calpain. *Nature* **405**, 360–364 (2000).
6. Bano, D. et al. Cleavage of the plasma membrane Na^+/Ca^{2+} exchanger in excitotoxicity. *Cell* **120**, 275–285 (2005).
7. Gan-Or, Z. et al. Mutations in CAPN1 cause autosomal-recessive hereditary spastic paraplegia. *Am. J. Hum. Genet.* **98**, 1271 (2016).
8. Wang, Y. et al. Defects in the CAPN1 gene result in alterations in cerebellar development and cerebellar ataxia in mice and humans. *Cell Rep.* **16**, 79–91 (2016).
9. Kanamori, T. et al. Compartmentalized calcium transients trigger dendrite pruning in Drosophila sensory neurons. *Science* **340**, 1475–1478 (2013).
10. Metwally, E., Zhao, G., Li, W., Wang, Q. & Zhang, Y. Q. Calcium-activated calpain specifically cleaves glutamate receptor IIA but not IIB at the Drosophila neuromuscular junction. *J. Neurosci.* **39**, 2776–2791 (2019).
11. Guroff, G. A neutral, calcium-activated proteinase from the soluble fraction of rat brain. *J. Biol. Chem.* **239**, 149–155 (1964).
12. Berridge, M. J., Bootman, M. D. & Roderick, H. L. Calcium signalling: dynamics, homeostasis and remodelling. *Nat. Rev. Mol. Cell Biol.* **4**, 517–529 (2003).
13. Clapham, D. E. Calcium signaling. *Cell* **131**, 1047–1058 (2007).
14. Chan, S. L. & Mattson, M. P. Caspase and calpain substrates: roles in synaptic plasticity and cell death. *J. Neurosci. Res.* **58**, 167–190 (1999).
15. Glading, A., Lauffenburger, D. A. & Wells, A. Cutting to the chase: calpain proteases in cell motility. *Trends Cell Biol.* **12**, 46–54 (2002).
16. Melloni, E. et al. Acyl-CoA-binding protein is a potent m-calpain activator. *J. Biol. Chem.* **275**, 82–86 (2000).
17. Lutas, A., Wahlmark, C. J., Acharjee, S. & Kawasaki, F. Genetic analysis in Drosophila reveals a role for the mitochondrial protein p32 in synaptic transmission. *G3. (Bethesda)* **2**, 59–69 (2012).
18. Xiao, K., Wang, Y., Chang, Z., Lao, Y. & Chang, D. C. p32, a novel binding partner of Mcl-1, positively regulates mitochondrial Ca(2+) uptake and apoptosis. *Biochem. Biophys. Res. Commun.* **451**, 322–328 (2014).
19. Koll, H. et al. Antifolding activity of hsp60 couples protein import into the mitochondrial matrix with export to the intermembrane space. *Cell* **68**, 1163–1175 (1992).
20. Yamamoto, H. et al. Tim50 is a subunit of the TIM23 complex that links protein translocation across the outer and inner mitochondrial membranes. *Cell* **111**, 519–528 (2002).
21. Cong, J., Goll, D. E., Peterson, A. M. & Kapprell, H. P. The role of autolysis in activity of the Ca2+-dependent proteinases (mu-calpain and m-calpain). *J. Biol. Chem.* **264**, 10096–10103 (1989).
22. Siman, R. & Noszek, J. C. Excitatory amino acids activate calpain I and induce structural protein breakdown in vivo. *Neuron* **1**, 279–287 (1988).
23. Sugiyama, S. et al. Involvement of the mitochondrial protein translocator component tim50 in growth, cell proliferation and the modulation of respiration in Drosophila. *Genetics* **176**, 927–936 (2007).
24. Chen, Y. et al. An efficient two-step subcellular fractionation method for the enrichment of insulin granules from INS-1 cells. *Biophys. Rep.* **1**, 34–40 (2015).
25. Lodish, H. et al. Molecular Cell Biology (4th edition, New York: W. H. Freeman press (2000).
26. Hood, J. L., Brooks, W. H. & Roszman, T. L. Differential compartmentalization of the calpain/calpastatin network with the endoplasmic reticulum and Golgi apparatus. *J. Biol. Chem.* **279**, 43126–43135 (2004).
27. Harbauer, A. B., Zahedi, R. P., Sickmann, A., Pfanner, N. & Meisinger, C. The protein import machinery of mitochondria—a regulatory hub in metabolism, stress, and disease. *Cell Metab.* **19**, 357–372 (2014).
28. Fukasawa, Y. et al. MitoFates: improved prediction of mitochondrial targeting sequences and their cleavage sites. *Mol. Cell Proteom.* **14**, 1113–1126 (2015).
29. Emanuelsson, O., Nielsen, H., Brunak, S. & von Heijne, G. Predicting subcellular localization of proteins based on their N-terminal amino acid sequence. *J. Mol. Biol.* **300**, 1005–1016 (2000).
30. Mossmann, D., Meisinger, C. & Vogtle, F. N. Processing of mitochondrial presequences. *Biochim. Biophys. Acta* **1819**, 1098–1106 (2012).

31. Vogtle, F. N. et al. Global analysis of the mitochondrial N-proteome identifies a processing peptidase critical for protein stability. *Cell* **139**, 428–439 (2009).
32. Shahrour, M. A. et al. Mitochondrial epileptic encephalopathy, 3-methylglutaconic aciduria and variable complex V deficiency associated with TIMM50 mutations. *Clin. Genet.* **91**, 690–696 (2017).
33. Leloup, L. et al. m-Calpain activation is regulated by its membrane localization and by its binding to phosphatidylinositol 4,5-bisphosphate. *J. Biol. Chem.* **285**, 33549–33566 (2010).
34. Meinecke, M. et al. Tim50 maintains the permeability barrier of the mitochondrial inner membrane. *Science* **312**, 1523–1526 (2006).
35. Collins, T. J., Berridge, M. J., Lipp, P. & Bootman, M. D. Mitochondria are morphologically and functionally heterogeneous within cells. *EMBO J.* **21**, 1616–1627 (2002).
36. Jekely, G. & Friedrich, P. Characterization of two recombinant Drosophila calpains. CALPA and a novel homolog, CALPB. *J. Biol. Chem.* **274**, 23893–23900 (1999).
37. Guo, Y. et al. Tim50, a component of the mitochondrial translocator, regulates mitochondrial integrity and cell death. *J. Biol. Chem.* **279**, 24813–24825 (2004).
38. Franco, S. J. & Huttenlocher, A. Regulating cell migration: calpains make the cut. *J. Cell Sci.* **118**, 3829–3838 (2005).
39. Moldoveanu, T. et al. A Ca(2+) switch aligns the active site of calpain. *Cell* **108**, 649–660 (2002).
40. Sorimachi, H., Hata, S. & Ono, Y. Impact of genetic insights into calpain biology. *J. Biochem.* **150**, 23–37 (2011).
41. Xu, W. et al. Calpain-mediated mGluR1alpha truncation: a key step in excitotoxicity. *Neuron* **53**, 399–412 (2007).
42. Luo, L. & O'Leary, D. D. Axon retraction and degeneration in development and disease. *Annu. Rev. Neurosci.* **28**, 127–156 (2005).
43. Losonczy, A., Makara, J. K. & Magee, J. C. Compartmentalized dendritic plasticity and input feature storage in neurons. *Nature* **452**, 436–441 (2008).
44. Fontenele, M. et al. Calpain A modulates Toll responses by limited Cactus/IkappaB proteolysis. *Mol. Biol. Cell* **24**, 2966–2980 (2013).
45. Bi, J. et al. Seipin promotes adipose tissue fat storage through the ER Ca(2)(+)-ATPase SERCA. *Cell Metab.* **19**, 861–871 (2014).
46. Gratz, S. J. et al. Highly specific and efficient CRISPR/Cas9-catalyzed homology-directed repair in Drosophila. *Genetics* **196**, 961–971 (2014).
47. Mao, C. X. et al. Microtubule-severing protein Katanin regulates neuromuscular junction development and dendritic elaboration in Drosophila. *Development* **141**, 1064–1074 (2014).
48. Zhao, G. et al. Drosophila S6 Kinase like inhibits neuromuscular junction growth by downregulating the BMP receptor thickveins. *PLoS Genet.* **11**, e1004984 (2015).
49. Palmer, A. E. & Tsien, R. Y. Measuring calcium signaling using genetically targetable fluorescent indicators. *Nat. Protoc.* **1**, 1057–1065 (2006).
50. Teodoro, R. O. et al. Ral mediates activity-dependent growth of postsynaptic membranes via recruitment of the exocyst. *EMBO J.* **32**, 2039–2055 (2013).
51. Wang, K. K. et al. An alpha-mercaptoacrylic acid derivative is a selective nonpeptide cell-permeable calpain inhibitor and is neuroprotective. *Proc. Natl. Acad. Sci. USA* **93**, 6687–6692 (1996).
52. Li, W. et al. Angelman syndrome protein Ube3a regulates synaptic growth and endocytosis by inhibiting bmp signaling in drosophila. *PLoS Genet.* **12**, e1006062 (2016).
53. Rogers, S. L. & Rogers, G. C. Culture of Drosophila S2 cells and their use for RNAi-mediated loss-of-function studies and immunofluorescence microscopy. *Nat. Protoc.* **3**, 606–611 (2008).
54. Dunn, K. W., Kamocka, M. M. & McDonald, J. H. A practical guide to evaluating colocalization in biological microscopy. *Am. J. Physiol. Cell Physiol.* **300**, 723–742 (2011).